2017

Photostability studies of retinyl palmitate entrapped in policosanol oleogel matrices

Yixing Tian
Iowa State University

Photostability studies of retinyl palmitate entrapped in policosanol oleogel matrices

by

Yixing Tian

A thesis submitted to the graduate faculty

in partial fulfillment of the requirements for the degree of

MASTER OF SCIENCE

Major: Food Science and Technology

Program of Study Committee:
Nuria Acevedo, Major Professor
Buddhi Lamsal
Wendy White

The student author, whose presentation of the scholarship herein was approved by the program of study committee, is solely responsible for the content of this thesis. The Graduate College will ensure this thesis is globally accessible and will not permit alterations after a degree is conferred.

Iowa State University

Ames, Iowa

2017

TABLE OF CONTENTS

Page

LIST OF TABLES

LIST OF FIGURES

Page

NOMENCLATURE

3D	Three Dimensional
AR	Anhydroretinol
BHA	3-tert-butyl-4-idroxi-anisole
BHT	Butylated Hydroxyl Toluene
CPMG	Carr-Purcell-Meiboom-Gill
DBS	1,3:2,4-di-*O*-benzylidene-*D*-sorbitol
DIC	Differential Interference Contrast
DMDBS	1,3:2,4-di-*Om*,*p*-dimethylbenzylidene-*D*-sorbitol
DSC	Differential Scanning Calorimetry
FA	Fatty Acid
FDA	Food and Drug Administration
FE-SEM	Field Emission Scanning Electron Microscopy
FOM	Fluorescent Optical Microscopy
HDL	High-Density Lipoprotein
HEC	Hydroxyethyl Cellulose
HPLC	High Performance Liquid Chromatography
LDL	Low-Density Lipoprotein
MDBS	1,3:2,4-di-*Op*-methylbenzylidene-*D*-sorbitol
NMR	^{1}H Nuclear Magnetic Resonance
O/W	Oil-in-Water
p-A.V.	p-Anisidine Value
PC	Policosanol

PCO	Policosanol Oleogel
PEG	Polyethylene Glycol 400
PV	Peroxide Value
RAE	Retinol Activity Equivalent
RDA	Recommended Dietary Allowance
RP	Retinyl Palmitate
SAFIN	Self-assembled Fibrillar Network
SLN	Solid Lipid Nanoparticle
SO	Soybean Oil
TEM	Transmission Electron Micrograph
THF	Tetrahydrofuran
UL	Upper intake Level

ACKNOWLEDGMENTS

I would like to thank my major professor, Dr. Acevedo, for your guidance, support and patience. I have learned a lot from you, not only how to be a food scientist, but also how to be a better person. Thank you for always believing in me and encouraging me. Thank you to my committee members, Dr. Wendy White and Dr. Buddhi Lamsal, for your guidance and support throughout the course of this research.

In addition, I would like to thank Dr. Ann Perera, Dr. Lucas Showman, and Dr. Kirthi Narayanaswamy, from W. M. Keck Metabolomics Research Laboratory for assisting with the HPLC method for retinyl palmitate analysis. Thank you to Dr. Eliseo De Leon for teaching me and helping me conduct DSC tests. Thank you to all of my labmates, Monica Primacella, Nicole Gaudino, John Fox, Shree Banjara, and Fei Tao, who provided me help and encouraged me all the time.

Thank you to my parents, sister, and close friends who always support me and encourage me to finish my graduate school. I would also like to thank my boyfriend, Zach, for your company and support.

ABSTRACT

Retinyl palmitate (RP) can easily lose its biological activity when exposed to ultraviolet radiation due to the UV-mediated degradation. There is a demand to explore new approaches to protect RP in an easy, economical and efficient way. Oleogels show a great potential to improve photostability of RP. The objective of this research was to determine the kinetics of RP photodegradation in policosanol oleogels (PCO) upon UVA exposure and the photoprotective mechanism of RP taking place in PCOs. Photostability of RP (0.04%, 0.1% and 1%, w/w) was studied in PCO matrices (7%, 10%, and 12%, w/w, policosanol in soybean oil) after UVA irradiation. PCOs efficiently protected RP from UVA-mediated degradation. Over 75% RP-activity remained in PCOs after 4 days of UVA irradiation, while only 12% RP-activity remained in soybean oil. HPLC analysis showed that *cis*-RP was formed in liquid soybean oil after 2 days of UVA irradiation while it was absent in PCOs matrices. For all samples, RP photodegradation followed a 2^{nd} order reaction. From the reaction kinetics, it would be possible to predict the RP photodegradation rate in PCO matrices. PCOs were shown to be a promising matrix to efficiently protect RP from photodegradation. PCOs can efficiently bock UVA energy absorption and further dampen the UVA mediated degradation. PCOs prepared at higher cooling rates had smaller crystal particle area sizes and provided better RP protection due to the molecular immobilization. Microscopies and matrix mobility results suggested that PCOs efficiently immobilized RP in the network and improved RP photostability by reducing molecular collisions. PV and p-A.V. results indicated that PCOs can improve oil oxidative stability and further hinder the progress of free radical-mediated reaction of RP.

CHAPTER 1. GENERAL INTRODUCTION

Thesis Organization

This thesis begins with a review of literature focusing on the protection of retinyl palmitate from photodegradation, including relevant information such as photoreaction of retinyl palmitate, strategies to protection retinyl palmitate, oleogels, oleogels as bioactive carrier and previous studies on policosanol oleogels. Tow manuscripts follow the literature review. Manuscript authors are part of the Department of Food Science and Human Nutrition. Dr. Acevedo is the author for correspondence for both manuscripts. This thesis ends with a conclusion and recommendation for future work.

Literature Review

Vitamin A

Vitamin A is a group of fat-soluble nutritional components that are essential for visual functions and maintenance of healthy epithelial tissues (Tanumihardjo, 2011). Various forms of vitamin A are available in human diet, including retinol, retinal, retinoic acid, and several provitamin A carotenoids (i.e. beta-carotene) (Wohl & Goodhart, 1960). The recommended dietary allowances (RDAs) for vitamin A are 900 mcg of retinol activity equivalents (RAE) for male adults (19+ years old) and 700 mcg RAE for female adults (Micronutrients, 2001). The food sources of vitamin A include milk, butter, egg yolk, liver and kidney (Coates, Blackman, Cragg, Levine, Moss, & White, 2004).

Deficiency of vitamin A can result in adverse effects on growth, reproduction, visual and immune system functions (Tee & Lee, 1992). Vitamin A deficiency is still a problem in developing countries, which leads to several symptoms, such as night blindness, xerophthalmia, dryness of skin, low resistance to infection (Sommer, 2008). The upper

intake levels (ULs) for preformed vitamin A are 3,000 mcg RAE for adults (19+ years old) and an excess intake of preformed vitamin A can cause significant toxicity, known as hypervitaminosis A (Coates, Blackman, Cragg, Levine, Moss, & White, 2004).

Retinyl Palmitate

Retinyl palmitate (RP), the ester of retinol and palmitic acid, is the major storage form of retinoid found in the retina, liver, skin, and intestine (Biesalski & Nohr, 2004). RP is a widely used ingredient in food products, medical treatment and cosmetics products, because it has better chemical and thermal stability than retinol (Ji & SEO, 1999). Environmental factors, including solvent, temperature and availability of oxygen, have important impact on the chemical stability of retinol and its esters (Deritter, 1982; Ji & SEO, 1999). Chemical decomposition pathways of retinol and its esters include thermal isomerization, dehydration and oxidation (Manan, Baines, Stone, & Ryley, 1995; McBee, Kuksa, Alvarez, de Lera, Prezhdo, Haeseleer, et al., 2000; Różanowska, Cantrell, Edge, Land, Sarna, & Truscott, 2005; Tolleson, Cherng, Xia, Boudreau, Yin, Wamer, et al., 2005). Isomerization from all-*trans* retinoids to its *cis*-isomers results in partial loss of vitamin A biological activity (Ball, 1998).

Photoreaction of Retinyl Palmitate

Previous study showed that RP is more stable to oxidation but more labile to photolysis than retinol (Ihara, Hashizume, Hirase, & SUZUE, 1999). Sunlight in both the UVA and UVB spectral regions can photoexcite retinol and its esters, produce a singlet excited state and mediate photochemical reactions (Fu, Xia, Yin, Cherng, Yan, Mei, et al., 2007). Photochemical reactions of retinoids include photoisomerization, photopolymerization, photooxidation and photodegradation (Crank & Pardijanto, 1995;

Magdeleine Mousseron-Canet, 1971; M Mousseron-Canet, Mani, Favie, & Lerner, 1966; Tsujimoto, Hozoji, Ohashi, Watanabe, & Hattori, 1984).

When exposed to UV light, all-*trans* retinol and its esters can easily form the less active *cis* isomers and degrade into harmful products such as reactive oxygen species (Xia, Yin, Wamer, Cherng, Boudreau, Howard, et al., 2006). In a previous study on the photoirradiation (365 nm) of RP in methanol, it was reported that photodecomposition products included palmitic acid, anhydroretinol (AR), 4,5-dihydro-5-methoxy-anhydroretinol and a dihydro-methoxy-anhydroretinol isomer (Tatariunas & Matsumoto, 2000). Cherng et al., (2005) conducted a study on the photodecomposition of RP in ethanol by UVA light and stated that the photoirradiation of RP was mediated by a light-initiated free radical chain reaction. These authors proposed that the identified photodecomposition products were formed through an ionic photodissociation mechanism and the photoirradiation of RP, 5,6-epoxy-RP and AR generated reactive oxygen species that led to lipid peroxidation. The photooxidation of photosensitized oxidation RP was considered to be initiated by singlet oxygen and produced AR and fragments derived from cleavage of the side-chain double bonds (Crank & Pardijanto, 1995).

Strategies to Protect Retinyl Palmitate

Several strategies haven been explored to improve photostability of RP. Carlotti et al., (2005) analyzed the photo and chemical stability of RP in an oil-in-water (O/W) emulsion and in solid lipid nanoparticles (SLN) introduced in the emulsion. SLNs provided physical UV-blocking action to RP in the emulsion. In this study, acetyl palmitate, glyceryl behenate, and palmitic acid SLNs, with RP, were prepared and introduced in an O/W emulsion. It was found that SLNs in O/W emulsion protected RP from photodegradation

induced by UVA and UVB. They also reported that nanoparticles can protect RP from thermal degradation.

SLNs (Preciro ATO5, Pluronic F68, sodium cholate) were developed as carrier system for RP (Carafa, Marianecci, Salvatorelli, Di Marzio, Cerreto, Lucania, et al., 2008). Surfactant mixture composition in SLNs was modified in order to reach better physical characteristics and vitamin entrapment efficiency. It was found that Preciro ATO5 SLN has a higher RP entrapment efficiency, but it was not able to prevent RP photodegradation. In this system, the addition of BHA (3-tert-butyl-4-idroxi-anisole) didn't improve RP photostability.

Pople and Singh (2006) investigated SLNs as a particulate carrier system to control the release of Vitamin A palmitate and improve skin hydration. The SLNs were prepared by high-pressure homogenization with a lipid phase, lipophilic surfactant sorbitan monooleate and distilled water. Vitamin A palmitate (25% of the lipid phase) was dispersed in the lipid phase. The transmission electron micrograph (TEM) of SLN dispersion showed that Vitamin A palmitate was entrapped in the spherical f nanoparticles and monolayer coating of surfactant on the nanoparticles surrounded the lipid core. The release of vitamin A palmitate at the end of 24 hours was slower from the conventional Carbopol gel (54.38%) than the nanoparticulate dispersion (67.52%). It was concluded that SLN was a promising particulate carrier with controlled drug release in skin.

Wang et al., (2012) reported that the photostability of entrapped RP was efficiently protected in supramolecular gels formed by self-assembly of sorbitol-based gelators in a solvent mixture of polyethylene glycol 400 (PEG400)/ethanol or 1,2-propylene glycol/ethanol. The results showed that among three sorbitol-based gelators in the study

(1,3:2,4-di-*O*-benzylidene-*D*-sorbitol (DBS), 1,3:2,4-di-*Op*-methylbenzylidene-*D*-sorbitol (MDBS) and 1,3:2,4-di-*Om*,*p*-dimethylbenzylidene-*D*-sorbitol (DMDBS)), the retained activity of RP in MDBS and DMDBS gels was better than that of DBS gels because of the extra methyl groups. With 0.4 wt% MDBS, it was found that the gel formed in oligomeric PEG400/ethanol (1/2, v/v) was slightly better in the RP protection than the gel formed by low molecular weight propylene glycol/ethanol (1/2, v/v), because the long chains of PEG entrapped RP molecules better. At different PEG400/ethanol ratios, the authors reported that RP photostability decreased with the decreasing content of PEG400. The experiments on the effect of RP concentrations ($1x10^{-2}$ mol/L, $2.5x10^{-3}$ mol/L, $2x10^{-4}$ mol/L) in MDBS gels indicated that the RP activity was retained the highest at 10^{-3} mol/L RP. After 80 min of UVA irradiation, 75% of RP activity was retained in MDBS gel, while only 10% was retained in the conventional polymeric hydroxyethyl cellulose (HEC) gel. The fluorescent optical microscopy (FOM) and field emission scanning electron microscopy (FE-SEM) images images of MDBS gels indicated that RP molecules were entrapped into the chambers without changing the three-dimensional network structures of gel. The similar UV spectra results of RP in MDBS gels and in the corresponding solution showed that chemical and physiological activity of RP were not affected by the physically entrapment in MDBS gels.

In another study, butylated hydroxyl toluene (BHT) was used as antioxidant in a study of Vitamin A stability under UVA and UVB radiation (Carlotti, Rossatto, & Gallarate, 2002). It was found that BHT improved the photostability of both retinol and RP in octyl octanoate solution. These results suggested that the degradation process in the solution followed an oxidative mechanism. BHT was reported to protect RP from both photo and

thermal degradation. RP was found to be more stable than retinol under UVA and UVB radiation.

Oleogels

Oleogel is a gel where the liquid phase is oil (Marangoni & Garti, 2011). Many organic molecules can be used as gelators to crystallize or further self-assemble to form a three dimensional (3D) network, which entraps liquid oil and form a solid-like gel system (Marangoni, 2012). Based on their gelling mechanisms, Dassanayake et al., (2011) grouped oleogel gelators in two categories: crystal particles system and self-assembly systems. Colloidal crystalline particles can form a network and entrap liquid oil inside. This colloidal crystalline network can be formed by gelators like diacylglycerols, monoacylglycerols, fatty acids, fatty alcohols and wax esters (Da Pieve, Calligaris, Nicoli, & Marangoni, 2010; Schaink, Van Malssen, Morgado-Alves, Kalnin, & Van der Linden, 2007; Toro-Vazquez, Morales-Rueda, Dibildox-Alvarado, Charó-Alonso, Alonzo-Macias, & González-Chávez, 2007). In a self-assembly system, a self-assembled fibrillar network (SAFIN) is formed. A clear example is phytosterol and oryzanol SAFIN network composed of helical and twisted crystalline ribbons (Rogers, Strober, Bot, Toro-Vazquez, Stortz, & Marangoni, 2014). During cooling, the formed phytosterol and oryzanol fibers self-assemble and grow into a 3D network, and entrap liquid oil in the network.

Oleogel has solid-like rheology behavior, which has great potential to replace the solid fat in food product (Marangoni, 2012). The physical properties of oleogels are greatly affected by the preparation method used, such as gelator concentration, cooling rate, and shear rate (Ojijo, Neeman, Eger, & Shimoni, 2004). In this way, oleogels can be engineered to reach specific characteristics, which makes them good candidates as potential replacers of

fats in foods (Blake & Marangoni, 2014). In 2015, the Food and Drug Administration (FDA) released the final determination stating partially hydrogenated oils are no longer Generally Recognized as Safe (GRAS) in human food ("Final Determination Regarding Partially Hydrogenated Oils (Removing *Trans* Fat)," 2015). FDA set 2018 as deadline to eliminate *trans* fats in the food supply ("Final Determination Regarding Partially Hydrogenated Oils (Removing T*rans* Fat)," 2015). Oleogels have great potential to be used in food industry to replace partially hydrogenated oils.

Oleogel as Bioactive Carrier

The application of oleogels in the food industry can reduce the use of saturated fat and hydrogenated oil. Oleogel can be used as delivery system for color, flavor, bioactive components and drugs (Marangoni, 2012). Lecithin organogel is the most investigated organogel for bioactive compounds delivery in food and cosmetic products. Lecithin and lipid phase can efficiently permeate membranes and deliver bioactive compounds like vitamin A (Raut, Bhadoriya, Uplanchiwar, Mishra, Gahane, & Jain, 2012). Lecithin can form fluid-filled reverse micellar structures and then self-assemble to form a three-dimensional networked structure. The amphiphilic property of lecithin contribute to the widely use of lecithin organogels as hydrophilic and hydrophobic bioactive compounds carriers (Avramiotis, Papadimitriou, Hatzara, Bekiari, Lianos, & Xenakis, 2007).

Other organogels also have been reported as bioactive compounds carriers, such as sorbitan monostearate oleogel (Almeida & Bahia, 2006), 12-hydroxystearic acid oleogel (Iwanaga, Sumizawa, Miyazaki, & Kakemi, 2010), and stearyl acrylate (Tokuyama & Kato, 2010). Amphiphilic molecules in gel-emulsion can self-assemble and form aggregates and entrap bioactive agents. Maiti et al. (2014) reported that gel-emulsions prepared with

amphiphiles buffer solutions and different solvents were used for the controlled release of entrapped vitamin B12. Seo and Chang (2005) investigated similar self-assembled amphiphiles (1H-imidazole) gel-emulsions as delivery system for the hydrophilic drug norfloxacin. They found that when the concentration of amphiphile increases, the stability of the gel improved. In a gel sate, the entrapment of norfloxacin was enhanced about 10 times compared with the tetrahydrofuran (THF)/n-hexane solution or sol state.

Policosanol

Policosanol (PC) is the common name for a mixture of high molecular weight fatty alcohols, mainly including docosanol (C22), tetracosanol (C24), hexacosanol (C26), octacosanol (C28), and triacontanol (C30) (Irmak, Dunford, & Milligan, 2006). The composition and content of PC depend on the extraction sources of PC, such as beeswax, sugar cane, wheat and rice bran wax (Dunford, Irmak, & Jonnala, 2010). In the US market, policosanol is widely used in commercially dietary supplements to help maintain cholesterol levels. It was reported that policosanol has positive effects on the prevention and treatment of cardiovascular diseases by lowering total and low-density lipoprotein (LDL) cholesterol levels and increasing high-density lipoprotein (HDL) cholesterol (Varady, Wang, & Jones, 2003). These authors also concluded that consuming 5 to 20 mg policosanol per day played an important role in decreasing the risk of atheroma formation by reducing platelet aggregation, endothelial damage, and foam cell formation. Gouni-Berthold and Berthold (2002) studied policosanol as a new lipid-lowering agent. They found that daily doses of 10 mg of policosanol can effectively lower total and LDL cholesterol with additional beneficial properties, including effects on smooth muscle cell proliferation, platelet aggregation, and LDL peroxidation. A significant decrease of arachidonic acid and collagen-induced platelet

aggregation in healthy volunteers after 2 weeks consumption of 10 mg/day policosanol was reported (Gouni-Berthold & Berthold, 2002). In another animal study, a daily intake of 1% (wt/wt) policosanol mixture with 96.3% ictacosanol for 12 weeks, octacosanol was found to have a significant positive correlation with the reduction in the levels of plasma triacylglycerol (Xu, Fitz, Riediger, & Moghadasian, 2007)

Previous Studies on Policosanol Oleogel

Long chain fatty acids (FA), fatty alcohols and their mixtures were able to form crystalline network with numerous small crystals to structure liquid to form oleogels by intermolecular hydrogen bonding (Daniel & Rajasekharan, 2003; Schaink, Van Malssen, Morgado-Alves, Kalnin, & Van der Linden, 2007). Daniel and Rajasekharan (2003) reported that the gelling ability of FA and alcohols were related to their chain lengths, carboxyl group, position of an additional hydroxyl group, and acyl chain length. In a previous study, Gandolfo, Bot and Floter (2004) used FA, fatty alcohols and their mixture to gel edible oils. These authors found that the hardness of oleogels were mainly influenced by the concentration gelator and ratio of FA and alcohols, regardless the type of vegetable oils.

Lupi, Gabriele, Greco, Baldino, Seta and de Cindio (2013) developed stable virgin olive oil based oleogels at different policosanol concentrations (0.1 to 55%, w/w). The policosanol was extracted from rice bran wax, with a total amount of 60% w/w of octacosanol. In their study, these authors indicated that 85℃ was a temperature high enough to prepare policosanol oleogels (PCO). It was also reported that the solid gel could be formed with a minimum 0.5% (w/w) policosanol as organogelator and that when increasing policosanol concentration, the difference between onset of crystallization temperature (T_{co}) and gelation temperature (T_g) became smaller, the gel strength increased.

In another study, Lupi et al., (2013) developed olive oil and policosanol organogels for drug (ferulic acid, 5% w/w) delivery purposes. They reported that the semisolid oleogels with 3% w/w policosanol were consistent and thermally stable for human ingestion. Furthermore, the *in-vitro* bioavailability and release studies showed that the presence of policosanol delayed the delivery of FA. These authors concluded that by changing the concentration of policosanol in the system, a desirable and efficient delivery system of FA can be achieved.

In a rheological study of stabilized meat sauces, PCOs and monoglycerides of fatty acids oleogel were used to replace fat (Francesca R Lupi, Gabriele, Seta, Baldino, & de Cindio, 2014). The authors of this study concluded that the oleogel had positive effects on the stability of meat sauces. And policosanol was found to be effective to improve stability.

Importance of this Research

The protection and delivery of RP study has been explored in O/W emulsion system (Carlotti, Rossatto, & Gallarate, 2002), nanostructured lipid carriers (Kong, Xia, & Liu, 2011), poly nanoparticles (Sane & Limtrakul, 2009), and supramolecular gels (Wang, Fang, Li, Fu, & Yang, 2012). Many of the Vitamin A protection strategies and systems are considered for cosmetic or pharmaceutical application; however, their performance applications in food applications are unknown (Loveday & Singh, 2008). The aforementioned strategies are still technologically challenging, such as labor intensity, high cost and low protection. Thus, there is still a need to explore efficient and economical approaches to protect vitamin A. Furthermore, there is a knowledge gap in the area of oleogels as an effective food grade protection and delivery system for bioactive components including RP. In addition, oleogel matrices are good candidates for potentially improving RP

photostability in both, food application and cosmetic or pharmaceutical applications. There is a lack of studies analyzing the structure and property of PCO. This study focuses on the characterizing PCO using different analytical methods and measuring the protection of RP in oleogel.

Project Structure

The first part of this project focused on the preparation and characterization of PCOs, and investigating the efficiency of the PCO matrices to protect RP. Different policosanol concentrations (7%, 10%, and 12%, w/w) were studied. Samples were treated with UVA light for different time to test RP photostability in PCO system. Rheometer, differential interference contrast microscope, differential scanning calorimetry, low resolution nuclear magnetic resonance, and high performance liquid chromatography were used to analyze the mechanical, structural and thermal properties of the systems as well as to quantify RP activity. The objective of the first part of this work was to investigate the effect of organogelator on the stability of RP in PCO matrices. It was hypothesized that PCO can efficiently protect RP from photodegradation.

The second part of study focused on exploring the mechanism of RP protection from degradation in the PCOs. Particularly, physical UV-blocking action, the effect of oleogel structure on protection, and retardation of free radical-mediated reactions were studied. It was hypothesized that PCOs can provide a physical UV-barrier for UVA radiation, immobilization of RP in the system and delay or hindering of free radical mediated reactions.

References

Almeida, I. F., & Bahia, M. F. (2006). Evaluation of the physical stability of two oleogels. International journal of pharmaceutics, 327(1), 73-77.

Avramiotis, S., Papadimitriou, V., Hatzara, E., Bekiari, V., Lianos, P., & Xenakis, A. (2007). Lecithin organogels used as bioactive compounds carriers. A microdomain properties investigation. Langmuir, 23(8), 4438-4447.

Ball, G. (1998). Vitamin A and the provitamin A carotenoids. In Bioavailability and Analysis of Vitamins in Foods, (pp. 115-161): Springer.

Biesalski, H. K., & Nohr, D. (2004). New aspects in vitamin A metabolism: the role of retinyl esters as systemic and local sources for retinol in mucous epithelia. The Journal of nutrition, 134(12), 3453S-3457S.

Blake, A. I., & Marangoni, A. G. (2014). Structure and physical properties of plant wax crystal networks and their relationship to oil binding capacity. Journal of the American Oil Chemists' Society, 91(6), 885-903.

Carafa, M., Marianecci, C., Salvatorelli, M., Di Marzio, L., Cerreto, F., Lucania, G., & Santucci, E. (2008). Formulations of retinyl palmitate included in solid lipid nanoparticles: characterization and influence on light-induced vitamin degradation. Journal of Drug Delivery Science and Technology, 18(2), 119-124.

Carlotti, M., Rossatto, V., & Gallarate, M. (2002). Vitamin A and vitamin A palmitate stability over time and under UVA and UVB radiation. International journal of pharmaceutics, 240(1), 85-94.

Carlotti, M., Sapino, S., Trotta, M., Battaglia, L., Vione, D., & Pelizzetti, E. (2005). Photostability and stability over time of retinyl palmitate in an O/W emulsion and in SLN introduced in the emulsion. Journal of dispersion science and technology, 26(2), 125-138.

Cherng, S.-H., Xia, Q., Blankenship, L. R., Freeman, J. P., Wamer, W. G., Howard, P. C., & Fu, P. P. (2005). Photodecomposition of retinyl palmitate in ethanol by UVA light formation of photodecomposition products, reactive oxygen species, and lipid peroxides. Chemical research in toxicology, 18(2), 129-138.

Coates, P. M., Blackman, M. R., Cragg, G. M., Levine, M., Moss, J., & White, J. D. (2004). Encyclopedia of dietary supplements: CRC Press.

Crank, G., & Pardijanto, M. S. (1995). Photo-oxidations and photosensitized oxidations of vitamin A and its palmitate ester. Journal of Photochemistry and Photobiology A: Chemistry, 85(1-2), 93-100.

Da Pieve, S., Calligaris, S., Nicoli, M. C., & Marangoni, A. G. (2010). Shear nanostructuring of monoglyceride organogels. Food Biophysics, 5(3), 211-217.

Daniel, J., & Rajasekharan, R. (2003). Organogelation of plant oils and hydrocarbons by long-chain saturated FA, fatty alcohols, wax esters, and dicarboxylic acids. Journal of the American Oil Chemists' Society, 80(5), 417-421.

Dassanayake, L. S. K., Kodali, D. R., & Ueno, S. (2011). Formation of oleogels based on edible lipid materials. Current opinion in colloid & interface science, 16(5), 432-439.

Deritter, E. (1982). Vitamins in pharmaceutical formulations. Journal of pharmaceutical sciences, 71(10), 1073-1096.

Dunford, N. T., Irmak, S., & Jonnala, R. (2010). Pressurised solvent extraction of policosanol from wheat straw, germ and bran. Food chemistry, 119(3), 1246-1249.

Final Determination Regarding Partially Hydrogenated Oils (Removing Trans Fat). In. (2015), vol. 2017): U.S. Food and Drug Administration.

Fu, P. P., Xia, Q., Yin, J. J., Cherng, S. H., Yan, J., Mei, N., Chen, T., Boudreau, M. D., Howard, P. C., & Wamer, W. G. (2007). Photodecomposition of vitamin A and

photobiological implications for the skin. Photochemistry and photobiology, 83(2), 409-424.
Gandolfo, F. G., Bot, A., & Flöter, E. (2004). Structuring of edible oils by long-chain FA, fatty alcohols, and their mixtures. Journal of the American Oil Chemists' Society, 81(1), 1-6.
Gouni-Berthold, I., & Berthold, H. K. (2002). Policosanol: clinical pharmacology and therapeutic significance of a new lipid-lowering agent. American heart journal, 143(2), 356-365.
Ihara, H., Hashizume, N., Hirase, N., & SUZUE, R. (1999). Esterification makes retinol more labile to photyolysis. Journal of nutritional science and vitaminology, 45(3), 353-358.
Irmak, S., Dunford, N. T., & Milligan, J. (2006). Policosanol contents of beeswax, sugar cane and wheat extracts. Food Chemistry, 95(2), 312-318.
Iwanaga, K., Sumizawa, T., Miyazaki, M., & Kakemi, M. (2010). Characterization of organogel as a novel oral controlled release formulation for lipophilic compounds. International journal of pharmaceutics, 388(1), 123-128.
Ji, H.-G., & SEO, B.-S. (1999). Retinyl palmitate at 5% in a cream: its stability, efficacy and effect. Cosmetics and toiletries, 114(3), 61-68.
Kong, R., Xia, Q., & Liu, G. Y. (2011). Preparation and characterization of vitamin A palmitate-loaded nanostructured lipid carriers as delivery systems for food products. In Advanced Materials Research, vol. 236 (pp. 1818-1823): Trans Tech Publ.
Loveday, S. M., & Singh, H. (2008). Recent advances in technologies for vitamin A protection in foods. Trends in food science & technology, 19(12), 657-668.
Lupi, F. R., Gabriele, D., Baldino, N., Mijovic, P., Parisi, O. I., & Puoci, F. (2013). Olive oil/policosanol organogels for nutraceutical and drug delivery purposes. Food & function, 4(10), 1512-1520.
Lupi, F. R., Gabriele, D., Greco, V., Baldino, N., Seta, L., & de Cindio, B. (2013). A rheological characterisation of an olive oil/fatty alcohols organogel. Food Research International, 51(2), 510-517.
Lupi, F. R., Gabriele, D., Seta, L., Baldino, N., & de Cindio, B. (2014). Rheological design of stabilized meat sauces for industrial uses. European Journal of Lipid Science and Technology, 116(12), 1734-1744.
Maiti, M., Roy, A., & Roy, S. (2014). Effect of pH and amphiphile concentration on the gel-emulsion of sodium salt of 2-dodecylpyridine-5-boronic acid: Entrapment and release of vitamin B 12. Colloids and Surfaces A: Physicochemical and Engineering Aspects, 461, 76-84.
Manan, F., Baines, A., Stone, J., & Ryley, J. (1995). The kinetics of the loss of all-trans retinol at low and intermediate water activity in air in the dark. Food Chemistry, 52(3), 267-273.
Marangoni, A. G. (2012). Organogels: an alternative edible oil-structuring method. Journal of the American Oil Chemists' Society, 89(5), 749-780.
Marangoni, A. G., & Garti, N. (2011). Edible oleogels: structure and health implications: Elsevier.
McBee, J. K., Kuksa, V., Alvarez, R., de Lera, A. R., Prezhdo, O., Haeseleer, F., Sokal, I., & Palczewski, K. (2000). Isomerization of all-trans-retinol to cis-retinols in bovine

retinal pigment epithelial cells: dependence on the specificity of retinoid-binding proteins. Biochemistry, 39(37), 11370.
Micronutrients, I. o. M. P. o. (2001). Dietary Reference Intakes for Vitamin A, Vitamin K, Arsenic, Boron, Chromium, Copper, Iodine, Iron, Manganese, Molybdenum, Nickel, Silicon, Vanadium, and Zinc: National Academies Press (US).
Mousseron-Canet, M. (1971). [242] Photochemical transformation of vitamin A. Methods in enzymology, 18, 591-615.
Mousseron-Canet, M., Mani, J., Favie, C., & Lerner, D. (1966). On the photochemical isomerization of vitamin A. Compt. Rend, 262, 153-155.
Ojijo, N. K., Neeman, I., Eger, S., & Shimoni, E. (2004). Effects of monoglyceride content, cooling rate and shear on the rheological properties of olive oil/monoglyceride gel networks. Journal of the Science of Food and Agriculture, 84(12), 1585-1593.
Pople, P. V., & Singh, K. K. (2006). Development and evaluation of topical formulation containing solid lipid nanoparticles of vitamin A. Aaps Pharmscitech, 7(4), E63-E69.
Raut, S., Bhadoriya, S. S., Uplanchiwar, V., Mishra, V., Gahane, A., & Jain, S. K. (2012). Lecithin organogel: A unique micellar system for the delivery of bioactive agents in the treatment of skin aging. Acta Pharmaceutica Sinica B, 2(1), 8-15.
Rogers, M. A., Strober, T., Bot, A., Toro-Vazquez, J. F., Stortz, T., & Marangoni, A. G. (2014). Edible oleogels in molecular gastronomy. International Journal of Gastronomy and Food Science, 2(1), 22-31.
Różanowska, M., Cantrell, A., Edge, R., Land, E. J., Sarna, T., & Truscott, T. G. (2005). Pulse radiolysis study of the interaction of retinoids with peroxyl radicals. Free Radical Biology and Medicine, 39(10), 1399-1405.
Sane, A., & Limtrakul, J. (2009). Formation of retinyl palmitate-loaded poly (l-lactide) nanoparticles using rapid expansion of supercritical solutions into liquid solvents (RESOLV). The Journal of Supercritical Fluids, 51(2), 230-237.
Schaink, H., Van Malssen, K., Morgado-Alves, S., Kalnin, D., & Van der Linden, E. (2007). Crystal network for edible oil organogels: possibilities and limitations of the fatty acid and fatty alcohol systems. Food Research International, 40(9), 1185-1193.
Seo, S. H., & Chang, J. Y. (2005). Organogels from 1 H-Imidazole Amphiphiles: Entrapment of a Hydrophilic Drug into Strands of the Self-Assembled Amphiphiles. Chemistry of materials, 17(12), 3249-3254.
Sommer, A. (2008). Vitamin A deficiency and clinical disease: an historical overview. The Journal of nutrition, 138(10), 1835-1839.
Tanumihardjo, S. A. (2011). Vitamin A: biomarkers of nutrition for development. The American journal of clinical nutrition, 94(2), 658S-665S.
Tatariunas, A., & Matsumoto, S. (2000). A retinyl palmitate model of the phenomenon of the intrinsic fluorescence increase in ceroid-lipofuscin cytosomes. Experimental gerontology, 35(9), 1327-1341.
Tee, E. S., & Lee, C. (1992). Carotenoids and retinoids in human nutrition. Critical Reviews in Food Science & Nutrition, 31(1-2), 103-163.
Tokuyama, H., & Kato, Y. (2010). Preparation of thermosensitive polymeric organogels and their drug release behaviors. European Polymer Journal, 46(2), 277-282.
Tolleson, W. H., Cherng, S.-H., Xia, Q., Boudreau, M., Yin, J. J., Wamer, W. G., Howard, P. C., Yu, H., & Fu, P. P. (2005). Photodecomposition and phototoxicity of natural

retinoids. International journal of environmental research and public health, 2(1), 147-155.

Toro-Vazquez, J., Morales-Rueda, J., Dibildox-Alvarado, E., Charó-Alonso, M., Alonzo-Macias, M., & González-Chávez, M. (2007). Thermal and textural properties of organogels developed by candelilla wax in safflower oil. Journal of the American Oil Chemists' Society, 84(11), 989-1000.

Tsujimoto, K., Hozoji, H., Ohashi, M., Watanabe, M., & Hattori, H. (1984). WAVELENGTH-DEPENDENT PEROXIDE FORMATION UPON IRRADIATION OF all-trans RETINAL IN AN AERATED SOLUTION. Chemistry Letters, 13(10), 1673-1676.

Varady, K. A., Wang, Y., & Jones, P. J. (2003). Role of policosanols in the prevention and treatment of cardiovascular disease. Nutrition reviews, 61(11), 376-383.

Wang, H., Fang, F., Li, X., Fu, C., & Yang, Y. (2012). Improved photostability of Vitamin A palmitate originating from self-assembled supramolecular gels. Chinese Science Bulletin, 57(33), 4257-4263.

Wohl, M. G., & Goodhart, R. S. (1960). Modern Nutrition in Health and Disease. Academic Medicine, 35(5), 463.

Xia, Q., Yin, J. J., Wamer, W. G., Cherng, S.-H., Boudreau, M. D., Howard, P. C., Yu, H., & Fu, P. P. (2006). Photoirradiation of retinyl palmitate in ethanol with ultraviolet light-formation of photodecomposition products, reactive oxygen species, and lipid peroxides. International journal of environmental research and public health, 3(2), 185-190.

Xu, Z., Fitz, E., Riediger, N., & Moghadasian, M. H. (2007). Dietary octacosanol reduces plasma triacylglycerol levels but not atherogenesis in apolipoprotein E–knockout mice. Nutrition research, 27(4), 212-217.

CHAPTER 2. KINETIC STUDY ON PHOTOSTABILITY OF RETINYL PALMITATE ENTRAPPED IN POLICOSANOL OLEOGELS

A paper submitted to *Food Chemistry*

Yixing Tian[1,2] and Nuria C. Acevedo[1*]

Abstract

Photostability of all-*trans* retinyl palmitate (RP) (100% bioactivity) was studied in policosanol oleogels (PCOs) matrices (7%, 10%, and 12%, w/w, policosanol in soybean oil) after UVA irradiation. RP was incorporated into PCOs at levels of 0.04%, 0.1% and 1% (w/w). PCOs efficiently protected RP from UVA-mediated degradation. Over 75% RP-activity remained in PCOs after 4 days of UVA irradiation, while only 12% RP-activity remained in soybean oil. HPLC analysis showed that *cis*-RP was formed in liquid soybean oil after 2 days of UVA irradiation while it was absent in PCOs matrices. PCOs blocked the energy absorption from UVA and further dampened the UVA-mediated ionic photodissociation and free radical reaction due to matrix immobilization. For all samples, RP photodegradation followed a 2nd order reaction. From the reaction kinetics, it would be possible to predict the RP photodegradation rate in PCO matrices. PCOs were shown to be a promising matrix to efficiently protect RP from photodegradation.

Introduction

Vitamin A is a group of nutritional components, including retinol, retinal, retinoic acid, and several provitamin A carotenoids (e.g. beta-carotene), that are essential for visual

[1] Department of Food Science and Human Nutrition, Iowa State University, Ames, IA 50011
[2] Primary researcher and author
[*] Author for correspondence

function and the maintenance of healthy epithelia tissues (skin, immune system, lungs, and others) (Coates, Blackman, Cragg, Levine, Moss, & White, 2004). Retinyl palmitate (RP) is an ester form of vitamin A and is widely used in food products, medical treatments and cosmetics products. However, RP is sensitive to UVA irradiation, which results in its photodegradation. Loveday and Singh (2008) summarized strategies for vitamin A protection based on the entrapment or encapsulation of vitamin A, including emulsion systems (Carlotti, Rossatto, & Gallarate, 2002; Flanagan & Singh, 2006; Yaghmur, De Campo, Sagalowicz, Leser, Glatter, Michel, et al., 2012), solid lipid nanoparticles (Carlotti, Sapino, Trotta, Battaglia, Vione, & Pelizzetti, 2005; Jenning & Gohla, 2001; Lim, Lee, & Kim, 2004), polymer encapsulation (Duclairoir, Irache, Nakache, Orecchioni, Chabenat, & Popineau, 1999; Jeong, Song, Kang, Ryu, Lee, Choi, et al., 2003; Çirpanli, ünlü, Çaliş, & Atilla Hincal, 2005), and addition of antioxidants (Carlotti, Rossatto, & Gallarate, 2002; Ihara, Hashizume, Hirase, & SUZUE, 1999; Yoshida, Sekine, Matsuzaki, Yanaki, & Yamaguchi, 1999).

However, the aforementioned strategies are technologically challenging. For instance, labor demands, cost and limited protection are some of the current drawbacks. Thus, there is a need to explore new approaches to protect vitamin A in an easy and economical way. Oleogels are a promising technology that can be appropriate for practical applications and health benefits. An oleogel is defined as a gel where the liquid phase is oil (Marangoni & Garti, 2011). Gelators can crystallize or self-assemble to form a 3D network, which entraps liquid oil in a solid-like gel system. The physical features of oleogels are greatly affected by the preparation method used, such as gelator concentration, as well as cooling and shear rate. Oleogels can be engineered to have desirable features and thus have the potential to be used

as delivery system for colorants, flavorings, bioactive components and drugs (Marangoni, 2012).

Policosanol (PC) is a mixture of long chain fatty alcohols, mainly including docosanol (C22), tetracosanol (C24), hexacosanol (C26), octacosanol (C28), and triacontanol (C30). Long chain fatty alcohols can self-assemble and form the three dimensional structure of an oleogel. Gandolfo, Bot, and Flöter (2004) reported that the hardness of fatty alcohols oleogels have an approximately positive relationship with the fatty alcohol concentration, and fatty alcohols yield harder oleogels than the same chain length fatty acids at the same concentration. F. R. Lupi, Gabriele, Greco, Baldino, Seta, and de Cindio (2013) found that a PC concentration between 2.5% and 3% (w/w) was enough to form a large number of crystals that aggregate into a 3D network. In another study, Francesca R Lupi, Gabriele, Baldino, Mijovic, Parisi, and Puoci (2013) reported that 3% policosanol organogels can be used as drug delivery system for ferulic acid (5% w/w).

The capacity of oleogel matrices to protect photolabile components has not been explored. We hypothesize that PCOs have great potential to prevent RP photodegradation. The objectives of this study were to investigate the effect of policosanol concentration in PCOs on RP photostability and to determine the kinetics of RP photodegradation upon UVA exposure. We chose to prepare PCOs at concentrations ranging between 7-12% (w/w) in order to ensure a desirable solid-like behavior of the gel systems. Concentrations of incorporated RP were chosen to ensure an appropriate RP amount in one serving of soybean oil (one tablespoon, 13.56g) based on the recommended daily allowance (RDA) and the upper level (UL) of vitamin A for adults, which is 900 µg retinol activity equivalents

(RAE)/day and 3000 μg/day of preformed vitamin A, respectively (National Academy Press, 2001).

Microstructure, mechanical and thermal properties, as well as oil binding capacity and matrix mobility of PCO matrices were analyzed. To evaluate the efficiency of PCO matrices to protect RP from photodegradation and to study the reaction kinetics, RP-PCOs were exposed to UVA radiation (365 nm) and the remaining *trans*-RP was subsequently analyzed by normal phase high performance liquid chromatography (HPLC).

Materials and methods

Materials

Soybean oil was generously provided by ADM oils (Decatur, IL, USA). 98% Policosanol containing 60% octacosanol was purchased from PureBulk Inc. (Roseburg, OR, USA). 2-Propanol (HPLC grade) and RP (1,600,000 – 1,800,000 USP units per gram) were obtained from Sigma-Aldrich (St. Louis, MO, USA). Hexane (HPLC grade) and ethyl ether were from Fisher Chemical (Fair Lawn, NJ, USA).

A UVA lamp Model ENF-280C (365 nm, 115V, 60Hz, 0.20 A) was used for UV irradiation treatment (Spectroline, NY, USA). The lamp provides 1.488×10^{-6} W/cm^2 measured by UV safety meter model 6D (Solar Light, Glenside, PA, USA).

Oleogel preparation

Policosanol (7, 10, 12%, w/w) was added to soybean oil. The samples were heated at 85 °C and stirred at 250 rpm for 30 minutes. Samples were cooled at 4°C with a cooling rate of 3°C/min and stored at 4 °C for one week before analysis. RP (0%, 0.04, 0.1%, and 1%, w/w) was added during the cooling stage while mixing. The range of RP concentration used was chosen based on RDA and UL requirements. For instance, one serving of PCOs with

0.04% RP can provide the RDA for vitamin A, while one serving of PCOs with 0.1% RP is the maximum dose without adverse effects as established by the UL. Samples with 1%RP in PCOs were also prepared with the aim of reaching higher concentrations with potential cosmetics applications.

Microstructure

Differential interference contrast (DIC) microscopy was used to analyze the microstructure of the PCOs. A small drop of liquid sample was placed between a preheated microscope slide and glass cover. The slides were subjected to a heating and cooling program to achieve the desired cooling rate (3℃/min) before observation. The images were acquired with a DIC microscope (Olympus BX53, Olympus Corporation, MA, USA) using the CellSens Dimension software (Olympus Corporation, MA, USA). 3 replicates were prepared and 10 images of each slide were recorded. The images were analyzed by using software ImageJ (NIH, MD, USA) to report crystal particle area (μm^2).

Oil binding capacity

To test the oil binding capacity of PCOs, discs were prepared by pouring the hot liquid oleogel mixture into PVC disc molds (22 mm diameter and 3.2 mm thickness). The samples were cooled in the molds to 4°C with a cooling rate of 3°C/min and stored at that temperature for a week before analysis. Each oleogel disc was removed from the mold, placed on a round filter paper (Whatman #5, 110 mm diameter) and incubated at 20 °C. The weight of each filter paper was recorded after 0, 24, and 48 hours of storage time. A filter paper without sample on it was used as control in the experiments to account for the environmental effect on the filter papers. Filter papers were large enough to absorb all the oil released from samples during the experiment without saturation. At least 10 replicates were

prepared and means and standard deviations are reported. Oil loss (%) was calculated by using the following equation:

$$\% \text{ Oil Loss} = \frac{[wt.paper\ (x\ h) - wt.paper\ (0\ h)] - [wt.blank\ (x\ h) - wt.blank\ (0\ h)]}{Total\ mass\ of\ sample} \times 100 \quad (1)$$

Mechanical Properties

The rheology behavior of the PCOs was studied with a Rheometer Haake RS 150 Rheostress (ThermosScientific, Waltham, USA). Sample discs were prepared as explained in the previous section with PVC molds (35 mm diameter, 3.2 mm thick). A 35 mm diameter serrated stainless steel plate (PP35Ti) was used for the measurements. To determine the linear viscoelastic region (LVR), an oscillatory stress sweep from 10 to 1,000 Pa at 20 °C was performed with a frequency of 1 Hz and normal force of 5 N. Storage modulus (G') and loss modulus (G") were determined from the stress sweep curves as the average value (in Pa) of the LVR. The yield stress (σ*) was calculated as the stress value (in Pa) when a reduction in G' of 10% was achieved. The complex modulus G* was calculated by using the following equation:

$$G^* = \sqrt{G'^2 + G"^2} \quad (2)$$

Mean values and standard deviations for at least 5 replicates are reported.

Thermal Properties

Analysis of the thermal properties of PCOs was carried out by differential scanning calorimetry (DSC, TA Instruments, New Castle, DE, USA). Samples were heated from 0 °C to 100 °C with a ramp of 5 °C/min, then held at 100 °C for 10 minutes and cooled to 0 °C at 5 °C/min. TA Universal Analysis software (TA Instruments, New Castle, DE, USA) was used to obtain melting temperature (T_m), gelation temperature (T_g), melting enthalpy (ΔH_m),

and gelation enthalpy (ΔH_g) from the thermograms. Means and standard deviations for at least 3 replicates are reported.

Matrix Molecular Mobility

Matrix mobility of PCOs were measured by ^1H nuclear magnetic resonance (NRM) spectrometery (Bruker Bio Spin Corporation, Billercia, MA, USA). Liquid samples were poured into flat-bottom glass NMR tube (10 mm diameter, 180 mm length) up to a height of 4 cm and cooled at 3 °C/min and afterwards stored at 4 °C for one week before testing. Each sample was prepared and analyzed in triplicate; means and standard deviations are reported.

The Carr-Purcell-Meiboom-Gill (CPMG) pulse sequence was used to measure spin-spin relaxation time (T_2) values between 0 and 1000 millisecond (ms). The separation between the 90° and 180° pulse was 1 tau and 600 data points were collected. A total of 8 scans were run with a 15.0 s recycle delay and gain of 60 dB. Relaxation curves were fitted to a continuous distribution of exponentials using the CONTIN algorithm (Bruker software, Bruker BioSpin Corporation, Billerica, MA).

RP photostability

Liquid RP-PCO mixtures were poured into plastic petri dishes (35 mm diameter and 4 mm height). The samples were cooled at 3 °C/min and stored at 4 °C for one week before UVA treatment. The RP-PCO dishes were placed directly under the UVA lamp (325 nm) at 10 cm distance. Equivalent liquid soybean oil with RP (0.04-1%, w/w) samples were used as controls. Samples were irradiated for 0, 0.5, 1, 2, 3, and 4 days. After UVA treatment, RP-PCO samples were transferred to HPLC amber vials and diluted with hexane to a RP concentration range from 0.01 to 0.1 mg/mL. At least two replicates of each samples were analyzed.

A method developed by Scalzo, Santucci, Cerreto, and Carafa (2004) with modifications was used to determine the residual concentration of *trans*-RP after UVA treatment by using normal phase high performance liquid chromatography (NP HPLC). The HPCL instrument (Agilent 1100 Series LC/MSD Ion Trap; Santa Clara, CA, USA) was equipped with a diode array detector (DAD) G1315B (Agilent, Santa Clara, CA, USA). Analyses were carried out with a 50 mm × 4.6 mm SUPELCOSIL™ LC-Si (5µm) column (Sigma-Aldrich, St. Louis, MO, USA). Mobile phase A hexane: isopropanol (99:1, v/v) and mobile phase B ethyl ether was used as mobile phase solvent. The amount of ethyl ether was increased from 0 to 5% (v/v) over 5 mins and then decreased to 0% during the following 2 mins. The flow rate was 1 mL/min and the sample injection volume was 10 µL. The detector was set at 325 nm and the reference wavelength was 360 nm.

The HPLC chromatogram was integrated by Quant analysis for 6300Series Ion Trap LC/MS version 1.8 (Agilent, Santa Clara, CA, USA). The remaining RP (%) was calculated by using the following equation:

$$\text{Remaining RP (\%)} = \frac{\text{peak area of RP (Xd UV)}}{\text{peak area of RP (0d UV)}} \times 100\% \quad (3)$$

Statistical analysis

Statistical analysis was carried out with Graph Pad Prism 5 (GraphPad Software, Inc., La Jolla, CA, USA). One-way analysis of variance (ANOVA) tests were conducted with Tukey's post test to adjust for multiple comparisions. Significant differences were defined as p-value < 0.05.

Results and Discussion

PCO concentrations of 7%, 10%, and 12% (w/w) were selected since they were able to form firm oleogels as shown in Figure **2.1**. 5% (w/w) PCO was also prepared resulting in

a weak oleogel network, thus, 5% PCO was only analyzed by DSC and was not further studied. As expected, the physical properties of PCOs were strongly influenced by the PC concentration in matrix. Gelator concentration played an important role in the network formation. In a virgin olive oil based PCOs study, Lupi, Gabriele, Greco, Baldino, Seta, and de Cindio (2013) reported that gelation can be observed at PC concentrations larger than a critical value between 0.3% and 0.5% (w/w). They analyzed the thermal and physical properties at low (2.5-3%, w/w) PC content oleogels; while our study primarily focused on higher concentration PCOs, which has potential to replace traditional commercial semi-solid or solid high-fat products, such as margarine or topical creams for edible or cosmetic applications, respectively.

PCOs Microstructure

PCOs microstructure was studied to establish the relationship between the observed physical properties and the morphology of the crystalline network in the system. Typical microscopy images of PCOs are shown in Figure **2.2**. 7% PCOs microstructure is characterized by large, needle-like crystals with a particle area of 148.3 ± 2.7 μm^2 (Figure **2.2** B), which are similar with the crystals in pure policosanol sample (Figure **2.2** A). At low concentration, crystals were formed and distributed far from another in the matrix without much interaction. As expected, higher PC concentration led to smaller crystal lengths as a result of the enhanced nucleation process (Acevedo, Block, & Marangoni, 2012). 10% PCOs had a crystal area of 133.6 ± 5.7 μm^2 and showed spherulitic-like supramolecular aggregates (Figure **2.2** C). Higher concentrations of PC in the matrix promoted the growth and expansion of the crystalline structure due to the higher supersaturation, which resulted in the formation of dense and big crystalline aggregates. As anticipated, 12% PCOs had similar

crystal morphology to that of 10% PCOs (Figure **2.2** D), however, 12% PCOs (55.0 ± 3.5 μm^2 crystal particle area) had smaller crystals than 7% and 10% PCOs, but showed complex crystalline aggregates structure with more branches. The microstructure of the 12% PCOs had more crystalline material with longer and more developed branches.

Oil binding capacity

Oil binding capacity is an important property of oleogels and can affect potential oleogel's application (Aguilera, Michel, & Mayor, 2004). The number, size, shape, and distribution of the crystals in the network are key factors to determine the oil binding capacity of the system (Omonov, Bouzidi, & Narine, 2010). Oil binding capacity of PCOs was analyzed through oil loss values (% OL) in order to determine the PCOs stability during short time storage.

The % OL values obtained from all of the PCOs as a function of time are shown in Figure **2.3**. As expected, PCOs with the lowest PC concentration (7%, w/w) showed the highest % OL due to the weak and under developed network formed at this PC ratio. This frail network was not able to entrap liquid oil effectively, which led to OL values of 11.0 ± 0.4% and 15.1 ± 0.7% after 24 and 48 hours of storage, respectively.

The % OL values for 10% PCOs (2.7 ± 0.2% and 3.2 ± 0.2% after 24 and 48 h of storage) were 75% lower than that for 7% PCOs due to the more stable network formed due to the higher PC concentration. As shown in the microscopy analysis of 7% PCOs (Figure **2.2** A), crystals are not able to aggregate to form a stable network with this low PC concentration. With higher PC ratio, i.e. the 10% PCOs matrix, larger crystals are formed with more branches and aggregates leading to a stronger 3D network which entraps liquid oil in the system. Thus, the higher the PCOs concentration, the lower the % OL values. The oil

binding capacity of PCOs or fatty alcohol oleogels has not been reported previously; however plant wax oleogels have crystal networks comparable to those of PCOs. For instance, in a plant wax study, Blake and Marangoni (2014) reported that an even distribution of crystals and a reduction in the size of crystals were correlated with a higher oil binding capacity. Surprisingly, the % OL values for 12% PCOs (3.9 ± 0.2% and 5.1 ± 0.3% after 24 and 48 hours of storage) were significantly higher ($p < 0.05$) than that for 10% PCOs. It is possible that after 48 hours the network of 12% PCO is still not properly developed to hold liquid oil as efficiently as 10% PCOs, leading to a transient higher %OL value. We thus conducted a long term oil loss test (up to 8 days). As expected, 12% PCOs had lower % OL values than the 10% PCOs over the long-term.

Rheological Properties

The mechanical properties of the different PCOs were analyzed by conducting normal force oscillatory stress sweep tests. The complex modulus (G*) and yield stress (σ*) values are shown in Figure **2.4**. It can be observed that, as expected, there was a significant increase in G* with the increase in PC concentration ($p < 0.05$), contributing to a stronger gel network with a more developed crystalline structure (Figure **2.2**) and resulting in a higher overall resistance to deformation. These results are in line with those of previous authors (Gandolfo, Bot, & Flöter, 2004; F. R. Lupi, Gabriele, Greco, Baldino, Seta, & de Cindio, 2013). The G* of these systems indicated their great potential to be used in applications requiring a semi-solid behavior. For example, in the food sector, G' or G* values for different spreadable products and margarine range between 25 kPa and 5 MPa (Vithanage, Grimson, & Smith, 2009). Therefore, it would be possible to engineer PCO with different PC concentrations in order to reach desirable rheological properties for food applications.

As shown in Figure **2.4** B, there was no significant difference in σ* values of 7% and 10% PCO ($p < 0.05$), while 12% PCO showed a significantly higher σ* ($p < 0.05$) indicating that a stronger force was required to introduce a permanent deformation in this matrix. The σ* value of 12% PCO was over four times the values of 7% PCO and 10% PCO. A similar difference in G* values was found between 12% PCO and 7% PCO. 10% PCO had a higher resistance to viscoelastic deformation (higher G* value) than 7% PCO, however they showed similar resistance to permanent deformation (σ*), suggesting that G* is more sensitive to changes in PC concentration than σ*. It is interesting to note that in general the rheological properties of PCOs follow the opposite trend found for % OL values when changing PC concentration except for 10 and 12% PCOs. In this study, the rheological parameters do not reflect the ability to retain oil for the 10% verse 12% PCOs matrices in which the organization of the microstructure, particularly the presence of vast open spaces in 12% PCOs, seems to be a more important consideration.

Thermal Properties

Melting point (T_m), gelation temperature (T_g), melting enthalpy (ΔH_m), and gelation enthalpy (ΔH_g) values are reported in Table **2.1**. Though no significant differences ($p < 0.05$) were observed in the T_m values of the 7 - 12% PCOs (63.1 ± 0.2 °C, 65.1 ± 0.1 °C, 65.2 ± 0.8 °C for 7, 10 and 12% PCOs), an increasing trend was observed when PC concentration increased. On the other hand, T_g increased when the PC concentration increased (57.1 ± 1.3 °C, 60.3 ± 0.2 °C, 60.1 ± 0.2 °C for 7, 10 and 12% PCOs). A similar tendency was found with ΔH_m and ΔH_g. These results reflect the more extensive branching of the oleogel network formed with higher concentrations of gelator (Abdallah, Lu, & Weiss, 1999). As mentioned above, 7% PCO formed a weak network when compared with PCOs with higher

PC ratio. With the increasing of PC ratio, larger crystals aggregates within a more developed structure were generated, thus higher energy (ΔH_g) was required to form those crystals. In order to reach the required energy, a higher temperature (T_g) was observed during gelation. Similar results were reported by Lupi, Gabriele, Greco, Baldino, Seta, and de Cindio (2013) for PCO samples. There were no significant differences between 10% and 12% PCOs, suggesting that a 2% increase in PC ratio did not significantly influence the systems' thermal properties.

Matrix mobility

The respective spin-spin relaxation times (T_2) spectra of soybean oil and different PCOs were measured to study the matrix mobility (Figure **2.5**). Shorter relaxation times indicate a greater degree of interactions with neighboring species and more crystalline network in the system, which associated with more physical molecular restriction and less solvent inclusions (Gravelle, Davidovich-Pinhas, Zetzl, Barbut, & Marangoni, 2016). The peak in each plot represents the proton pool population that has similar mobility. Overall, soybean oil had a higher T_2 value than PCOs regardless of the PC ratio, which is associated with a lower molecular mobility in PCOs. The increase in PC concentration from 0% to 12% (w/w) resulted in a decrease in T_2 values, suggesting that molecular restriction of soybean oil by interaction with PC lowered the molecular mobility in the system. These findings are consistent with a previous study on 12-hydroxystearic acid organogels ((Rogers, Wright, & Marangoni, 2009). The authors found that with the increase of 12-hydroxystearic acid concentration in the system, the T_2 relaxations decreased, which indicated that the increase in the gelator concentration led to an increase in the confinement of the liquid oil. Gravelle, Davidovich-Pinhas, Zetzl, Barbut and Marangoni (2016) found that stronger ethylcellulose

oleogels had shorter T2 relaxation times due to the greater interaction between solvent and polymer. Overall, the NMR results support the oil loss and rheology results presented above.

Studies of RP-photostability in PCO matrices

All-*trans* RP is sensitive to UVA which mediates its degradation or isomerization (Scalzo, Santucci, Cerreto, & Carafa, 2004). The biological activity of *cis*-isomers of RP is less than that of all-*trans* RP; i.e. all-*trans* RP shows 100% biological activity, while biological activity for 13-*cis* isomer is 75% and for 9-*cis* isomer is 25% (Jung, Lee, & Kim, 1998).

In this study, 1% all-*trans* RP in soybean oil (RP-SO) was used as a control. One peak was observed in the chromatograms (Figure **2.6** A, peak a), which corresponds to all-*trans* RP. After one day of UVA irradiation, an additional peak was observed in the chromatogram corresponding to 9-*cis* RP (Figure **2.6** A, peak b) (Murphy, Engelhardt, & Smith, 1988). With the increase of the duration of UVA irradiation, the area of peak b increased, while that of peak a decreased. These results suggest that UVA mediated the isomerization of all-*trans* RP over time, becoming significant after one day of treatment.

The NP-HPLC chromatograms obtained for all the 1% RP-PCOs samples are shown in Figure 3. All-*trans* RP was found in all RP-PCOs. The formation of 9-*cis* RP was not found in PCOs, suggesting that PCOs protected all-*trans* RP from isomerization. In 7% PCOs, the peak area gradually decreased with an increase in UVA treatment time (Figure **2.6**B). The same trend was also found in 12% PCOs (Figure **2.6** D). However, in 10% PCOs (Figure **2.6** C), the all-*trans* RP peak decreased significantly upon 0.5 days of UVA treatment followed by a stabilization at longer irradiation time.

The efficiency of RP protection from photodegradation in all PCOs are compared in Figure **2.7**. The curves of the % remaining RP for 7% PCOs and 12% PCOs are similar and follow a decreasing linear trend with increasing UVA irradiation time. The % remaining RP values in 7% and 12% PCOs are significantly higher than those in 10% PCO and SO regardless the UV irradiation time. The % remaining RP in 10% PCO significantly decreased within the first 0.5 day of UVA irradiation and no further significant decrease was observed at longer irradiation time. Overall, 55% RP activity remained in 10% PCOs, and over 75% RP-activity was preserved in 7% and 12% PCOs after 4 days of UVA irradiation. On the other hand, the remaining RP activity in liquid SO was only 12%. 10% PCOs can significantly protect RP from photodegradation compared with liquid SO, but not as efficiently as 7% and 12% PCOs. The difference in RP protection can be attributed to the fact that 10% PCOs can retain more liquid oil in the system (lower %OL), but the network is not sufficiently developed to exert a noticeable protective effect; particularly at short time when it seems the network is still consolidating its structure. Overall, these results suggest that due to its inherent crystalline structure PCOs blocked the energy absorption from UVA and further dampened the UVA mediated photodegradation of RP (ionic photodissociation and free radical-mediated reaction) probably due to matrix immobilization.

Previous authors (Semenzato, Bau, Dall'Aglio, Nicolini, Bettero, & Calliari, 1994) stated that the RP stability in an emulsion depends on the presence of a coherent gel-like structure. Wang, Fang, Li, Fu, and Yang (2012) found that RP-photostability can be improved in sorbitol-based gels. The authors concluded that the three-dimensional network structure formed by the self-assembly of the gelators contributed to the protection of RP through reducing the molecular collisions and the degradation process. However, the UVA

irradiation treatment was not clearly described in this paper. Thus, it is difficult to compare their results with our study.

When studying the incorporation of different RP concentrations into PCOs, 7% (Figure **2.7** B) and 12% PCOs (Figure **2.7** D) presented the same trend, i.e. the protection was more efficient with higher concentrations of RP. Previous studies (Allwood & Plane, 1986) on photostability of RP have reported that the degradation rate is related to the initial RP concentration, where higher RP concentration leads to lower reaction rate, thus enhancing RP protection. However, this trend was not clear in 10% PCOs (Figure **2.7** C) due to the low protection efficiency in this matrices. Concentrations of 1% and 0.1% RP in these PCOs presented similar % remaining RP after 4 days of UVA treatment. The % remaining RP values for 0.04% RP were the lowest for 10% PCOs; however these were much higher than the control.

Kinetics of RP photodegradation

With the results obtained from the chromatograms, it was possible to obtain the kinetics of RP photodegradation in PCOs as seen in Figure **2.8**. It was found that the photodegradation of RP followed a 2^{nd} order reaction, regardless the PC or RP concentration used to prepare the oleogels. From the linear trend lines, the kinetics equations and the rate constant values, k, for each sample were obtained. Considering the kinetics results, it is possible to see that the rate constants (k) are higher in PCOs with less added RP, demonstrating a decreasing trend in RP-photostability when RP concentrations decline from 1% to 0.04%. These results are in line with a previous study where was reported that RP-degradation in ethanol and octyl octanoate solutions depends inversely on their initial molar concentration (Carlotti, Rossatto, & Gallarate, 2002). To clearly depict this effect, k values

as a function of initial concentration of RP (C_0) were plotted (Figure **2.9** A). Again, with the increase of initial RP concentration, the k value decreases, which indicates that the photodegradation rate is slower. When plotting the logarithm of k as a function of the reciprocal of C_0 (Figure **2.9** B), linear trend can be obtained for each PCO sample. Therefore, from the obtained linear equation, with a known initial concentration of RP, it could be possible to predict the photodegradation rate in PCOs. At lower k values, 7% PCO and 12%PCO can provide better protection than 10%PCO.

Conclusion

This study focused on the characterization of semi-solid PCOs and PCOs as matrix to protect RP from UVA mediated photodegradation. The PC concentration played an important role in the formation and characteristics of PCOs and RP protection. With the increase of PC concentration, the gelation temperature and gel strength increased, where matrix mobility decreased (T_2 decreased).These characteristics demonstrated the potential of PCOs as semisolid material capable to provide desirable consistency. It was found that PCOs efficiently protected RP from UVA-mediated degradation. The remaining RP activity in PCOs significantly decreased within the first 0.5 day of UVA irradiation and decreased slowly after that. Over 75% of RP activity remained after 4 days of UVA irradiation in 7% PCO and 12% PCO, while RP activity in liquid soybean oil was only 12%. HPLC analysis showed that *cis*-RP, with less than 75% all *trans*-RP activity, was formed only in liquid soybean oil after 2 days of UVA irradiation, while it was not found in PCOs. The results suggested that PCOs blocked the energy absorption from UVA and further dampened the UVA mediated photoirradiation of RP (ionic photodissociation and free radical reaction) due to matrix immobilization. From the reaction kinetics, it would be possible to predict the RP

photodegradtion rate in PCO matrices. The larger the amount of RP added into PCO matrices the more effective the photoprotection exerted by PCOs.

PCO is an efficient oil-structuring strategy to improve RP-photostability with the advantages of low cost, system stability and ease of preparation. PCOs enriched in RP have shown functional properties that are desirable for food and cosmetic applications.

References

Abdallah, D. J., Lu, L., & Weiss, R. G. (1999). Thermoreversible organogels from alkane gelators with one heteroatom. Chemistry of materials, 11(10), 2907-2911.

Acevedo, N. C., Block, J. M., & Marangoni, A. G. (2012). Critical laminar shear-temperature effects on the nano-and mesoscale structure of a model fat and its relationship to oil binding and rheological properties. Faraday discussions, 158(1), 171-194.

Aguilera, J., Michel, M., & Mayor, G. (2004). Fat migration in chocolate: diffusion or capillary flow in a particulate solid?—a hypothesis paper. Journal of Food Science, 69(7), 167-174.

Allwood, M., & Plane, J. (1986). The wavelength-dependent degradation of vitamin A exposed to ultraviolet radiation. International journal of pharmaceutics, 31(1-2), 1-7.

Blake, A. I., & Marangoni, A. G. (2014). Structure and physical properties of plant wax crystal networks and their relationship to oil binding capacity. Journal of the American Oil Chemists' Society, 91(6), 885-903.

Carlotti, M., Rossatto, V., & Gallarate, M. (2002). Vitamin A and vitamin A palmitate stability over time and under UVA and UVB radiation. International journal of pharmaceutics, 240(1), 85-94.

Carlotti, M., Sapino, S., Trotta, M., Battaglia, L., Vione, D., & Pelizzetti, E. (2005). Photostability and stability over time of retinyl palmitate in an O/W emulsion and in SLN introduced in the emulsion. Journal of dispersion science and technology, 26(2), 125-138.

Coates, P. M., Blackman, M. R., Cragg, G. M., Levine, M., Moss, J., & White, J. D. (2004). Encyclopedia of dietary supplements: CRC Press.

Duclairoir, C., Irache, J. M., Nakache, E., Orecchioni, A. M., Chabenat, C., & Popineau, Y. (1999). Gliadin nanoparticles: formation, all-trans-retinoic acid entrapment and release, size optimization. Polymer international, 48(4), 327-333.

Flanagan, J., & Singh, H. (2006). Microemulsions: a potential delivery system for bioactives in food. Critical reviews in food science and nutrition, 46(3), 221-237.

Gandolfo, F. G., Bot, A., & Flöter, E. (2004). Structuring of edible oils by long-chain FA, fatty alcohols, and their mixtures. Journal of the American Oil Chemists' Society, 81(1), 1-6.

Gravelle, A., Davidovich-Pinhas, M., Zetzl, A., Barbut, S., & Marangoni, A. (2016). Influence of solvent quality on the mechanical strength of ethylcellulose oleogels. Carbohydrate polymers, 135, 169-179.

Ihara, H., Hashizume, N., Hirase, N., & SUZUE, R. (1999). Esterification makes retinol more labile to photyolysis. Journal of nutritional science and vitaminology, 45(3), 353-358.

Jenning, V., & Gohla, S. H. (2001). Encapsulation of retinoids in solid lipid nanoparticles (SLN). Journal of microencapsulation, 18(2), 149-158.

Jeong, Y.-I., Song, J.-G., Kang, S.-S., Ryu, H.-H., Lee, Y.-H., Choi, C., Shin, B.-A., Kim, K.-K., Ahn, K.-Y., & Jung, S. (2003). Preparation of poly (DL-lactide-co-glycolide) microspheres encapsulating all-trans retinoic acid. International journal of pharmaceutics, 259(1), 79-91.

Jung, M., Lee, K., & Kim, S. (1998). Retinyl palmitate isomers in skim milk during light storage as affected by ascorbic acid. Journal of food science, 63(4), 597-600.

Lim, S.-J., Lee, M.-K., & Kim, C.-K. (2004). Altered chemical and biological activities of all-trans retinoic acid incorporated in solid lipid nanoparticle powders. Journal of controlled release, 100(1), 53-61.

Loveday, S. M., & Singh, H. (2008). Recent advances in technologies for vitamin A protection in foods. Trends in food science & technology, 19(12), 657-668.

Lupi, F. R., Gabriele, D., Greco, V., Baldino, N., Seta, L., & de Cindio, B. (2013). A rheological characterisation of an olive oil/fatty alcohols organogel. Food Research International, 51(2), 510-517.

Marangoni, A. G. (2012). Organogels: an alternative edible oil-structuring method. Journal of the American Oil Chemists' Society, 89(5), 749-780.

Marangoni, A. G., & Garti, N. (2011). Edible oleogels: structure and health implications: Elsevier.

Murphy, P. A., Engelhardt, R., & Smith, S. E. (1988). Isomerization of retinyl palmitate in fortified skim milk under retail fluorescent lighting. Journal of agricultural and food chemistry, 36(3), 592-595.

Omonov, T. S., Bouzidi, L., & Narine, S. S. (2010). Quantification of oil binding capacity of structuring fats: A novel method and its application. Chemistry and physics of lipids, 163(7), 728-740.

Rogers, M. A., Wright, A. J., & Marangoni, A. G. (2008). Post-crystallization increases in the mechanical strength of self-assembled fibrillar networks is due to an increase in network supramolecular ordering. Journal of Physics D: Applied Physics, 41(21), 215501.

Rogers, M. A., Wright, A. J., & Marangoni, A. G. (2009). Nanostructuring fiber morphology and solvent inclusions in 12-hydroxystearic acid/canola oil organogels. Current opinion in colloid & interface science, 14(1), 33-42.

Scalzo, M., Santucci, E., Cerreto, F., & Carafa, M. (2004). Model lipophilic formulations of retinyl palmitate: influence of conservative agents on light-induced degradation. Journal of pharmaceutical and biomedical analysis, 34(5), 921-931.

Semenzato, A., Bau, A., Dall'Aglio, C., Nicolini, M., Bettero, A., & Calliari, I. (1994). Stability of vitamin A palmitate in cosmetic emulsions: influence of physical parameters. International journal of cosmetic science, 16(4), 139-147.

Vithanage, C. R., Grimson, M. J., & Smith, B. G. (2009). The effect of temperature on the rheology of butter, a spreadable blend and spreads. Journal of texture studies, 40(3), 346-369.

Wang, H., Fang, F., Li, X., Fu, C., & Yang, Y. (2012). Improved photostability of Vitamin A palmitate originating from self-assembled supramolecular gels. Chinese Science Bulletin, 57(33), 4257-4263.

Yaghmur, A., De Campo, L., Sagalowicz, L., Leser, M., Glatter, O., Michel, M., & Watzke, H. J. (2012). Oil-in-water emulsion for delivery. In): Google Patents.

Yoshida, K., Sekine, T., Matsuzaki, F., Yanaki, T., & Yamaguchi, M. (1999). Stability of vitamin A in oil-in-water-in-oil-type multiple emulsions. Journal of the American Oil Chemists' Society, 76(2), 1-6.

Çirpanli, Y., ünlü, N., Çaliş, S., & Atilla Hincal, A. (2005). Formulation and in-vitro characterization of retinoic acid loaded poly (lactic-co-glycolic acid) microspheres. Journal of microencapsulation, 22(8), 877-889.

Table 2.1 Melting point (T_m), gelation temperature (T_g), melting enthalpy (ΔH_m), and gelation enthalpy (ΔH_g) values of 5%, 7%, 10%, and 12% (w/w) PCOs. Different letters represent statistically differences between values across all samples ($p < 0.05$).

	5% PCO	7% PCO	10% PCO	12% PCO
T_m (°C)	60.6 ^{a} ± 0.8	63.1 ^{b} ± 0.2	65.1 ^{b} ± 0.1	65.2 ^{b} ± 0.8
ΔH_m (J/g)	11.2 ^{a} ± 1.2	16.2 ^{b} ± 2.6	22.1 ^{c} ± 0.4	25.7 ^{c} ± 0.8
T_g (°C)	53.0 ^{a} ± 0.9	57.1 ^{b} ± 1.3	60.3 ^{c} ± 0.2	60.1 ^{c} ± 0.2
ΔH_g (J/g)	14.2 ^{a} ± 0.2	21.2 ^{b} ± 1.3	29.5 ^{c} ± 1.7	32.6 ^{c} ± 1.1

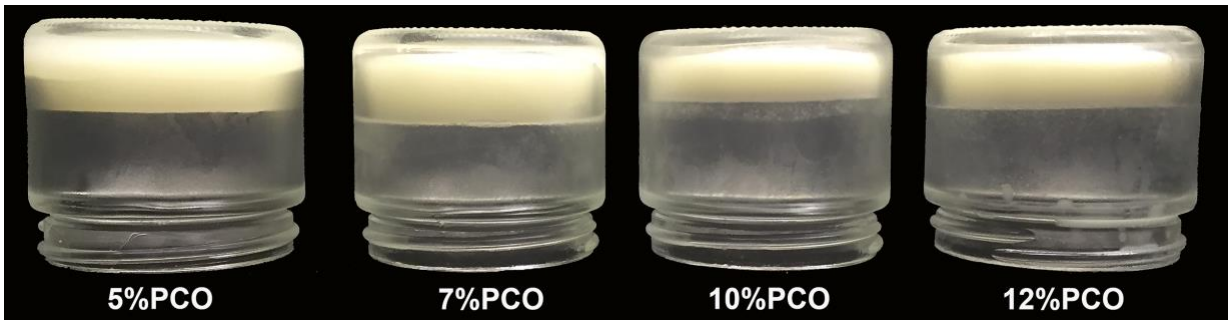

Figure 2.1 PCOs prepared with different concentration of policosanol

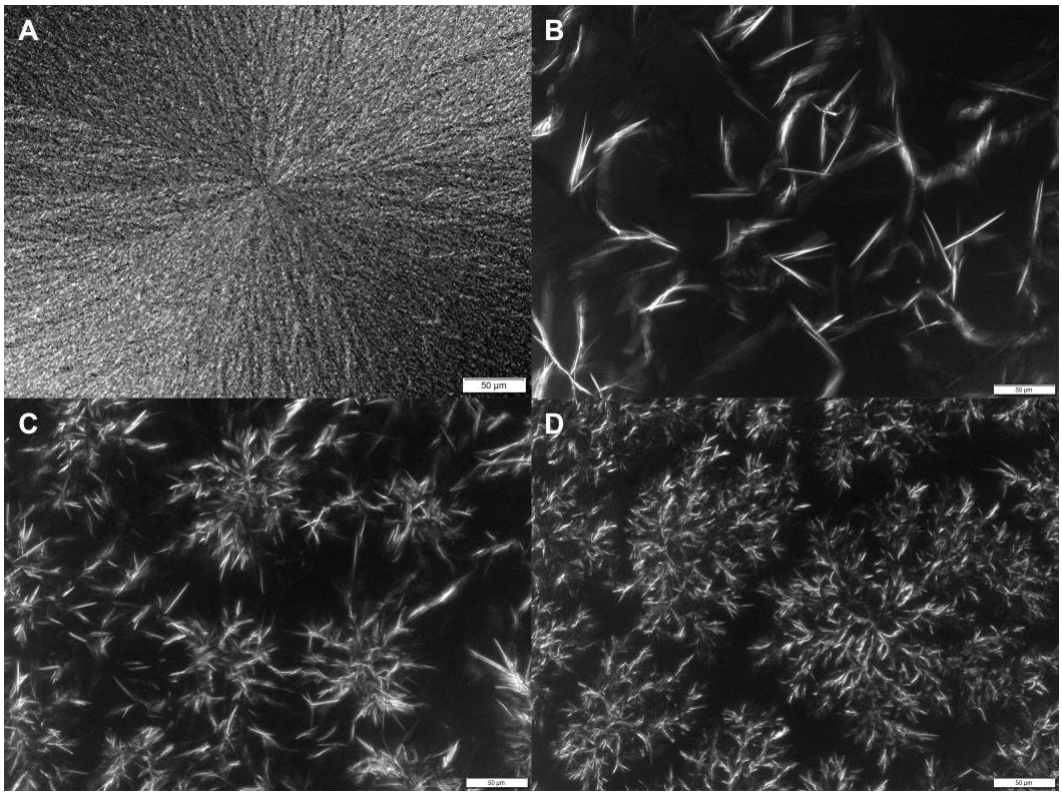

Figure 2.2 Micrographs obtained by DIC microscope of different PCOs. (A) Policosanol (B) 7%PCO (w/w) (C) 10% PCO (w/w) (D) 12% PCO (w/w)

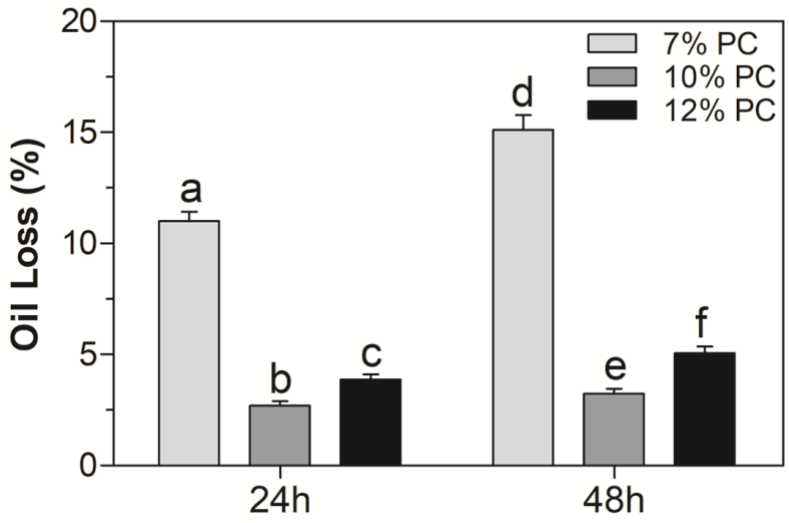

Figure 2.3 Oil loss values (% OL) for 7%, 10%, and 12% (w/w) PCOs. Different letters assigned to each bar represent statistically significant differences between the values across all samples ($p < 0.05$).

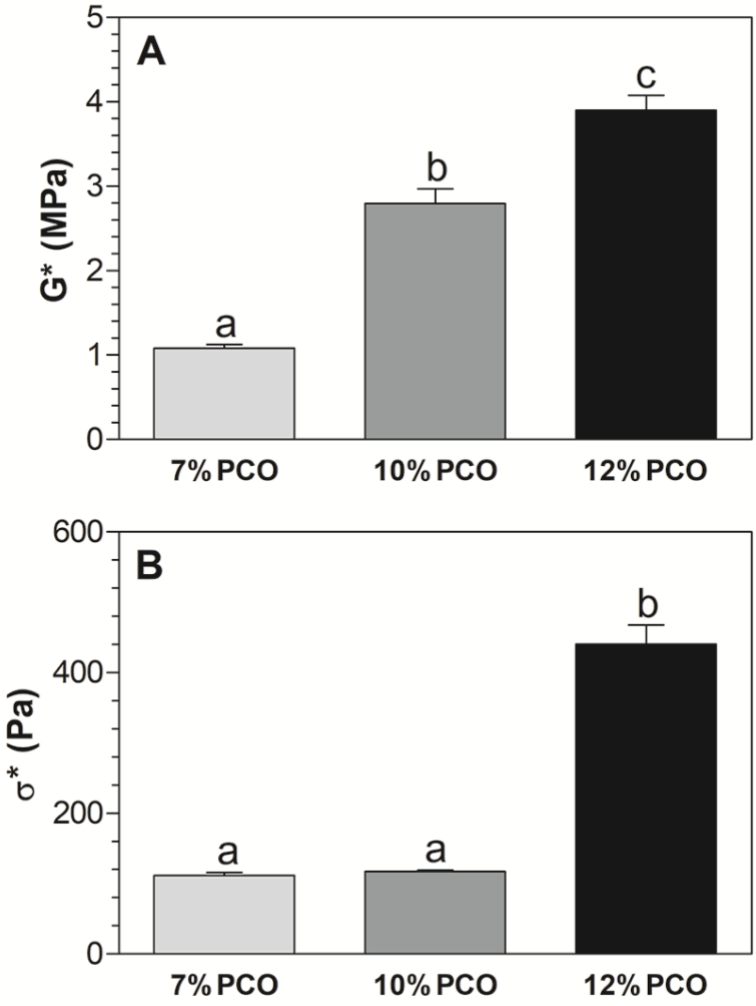

Figure 2.4 (A) Complex modulus (G*) and (B) yield stress (σ*) values for 7%, 10%, and 12% (w/w) PCOs. Different letters assigned to each bar represent statistically significant differences between samples ($p < 0.05$).

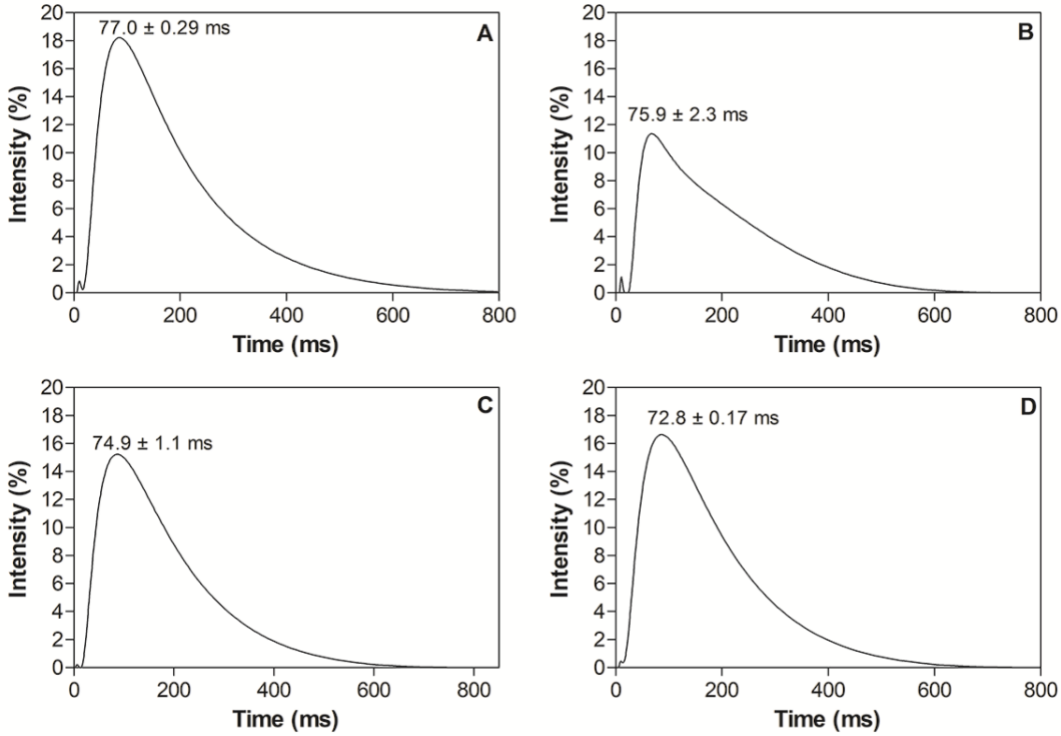

Figure 2.5 NMR T_2 relaxation spectra of the PCO samples. (A) soybean oil (B) 7% PCO (C) 10% PCO (D) 12% PCO.

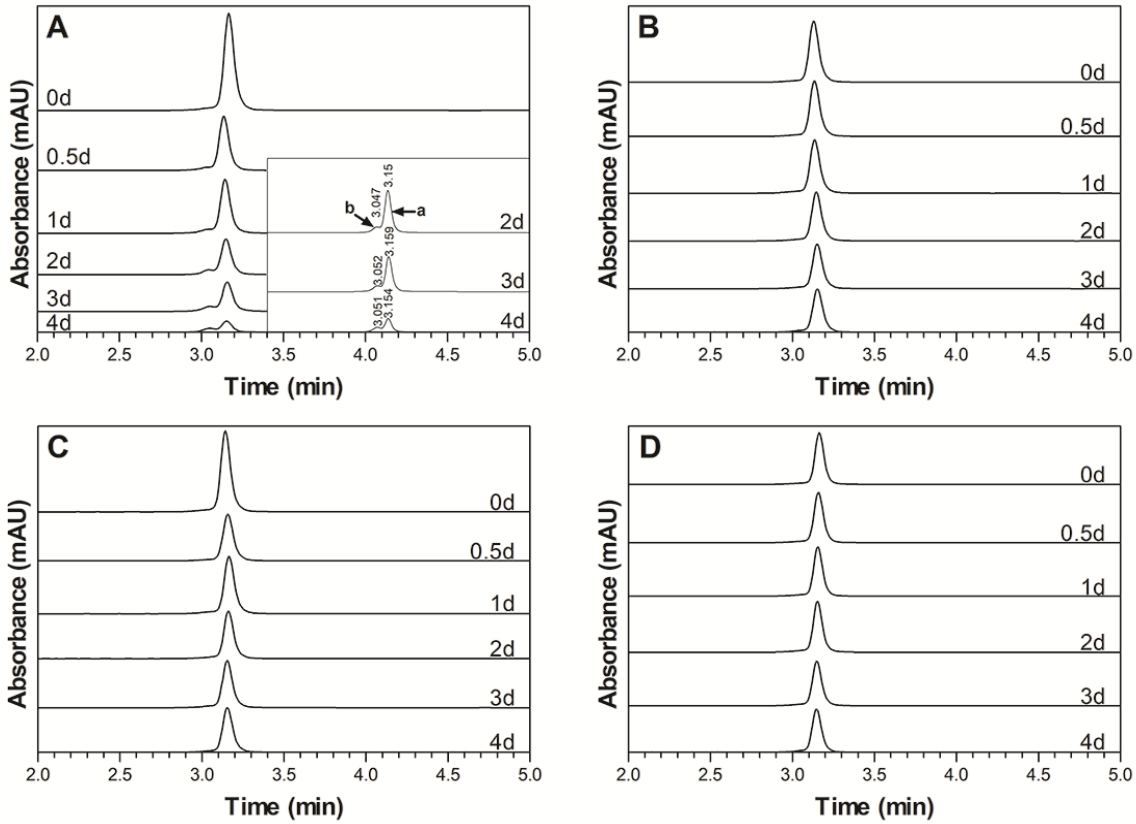

Figure 2.6 HPLC chromatograph of RP after different times (0, 0.5, 1, 2, 3, 4 days) of UVA radiation. (A) 1% RP in soybean oil, peak a and b correspond to all-*trans* and 9-*cis* RP, respectively (B) 1%RP in 7% PCOs (C) 1%RP in 10% PCOs (D) 1%RP in 12% PCOs

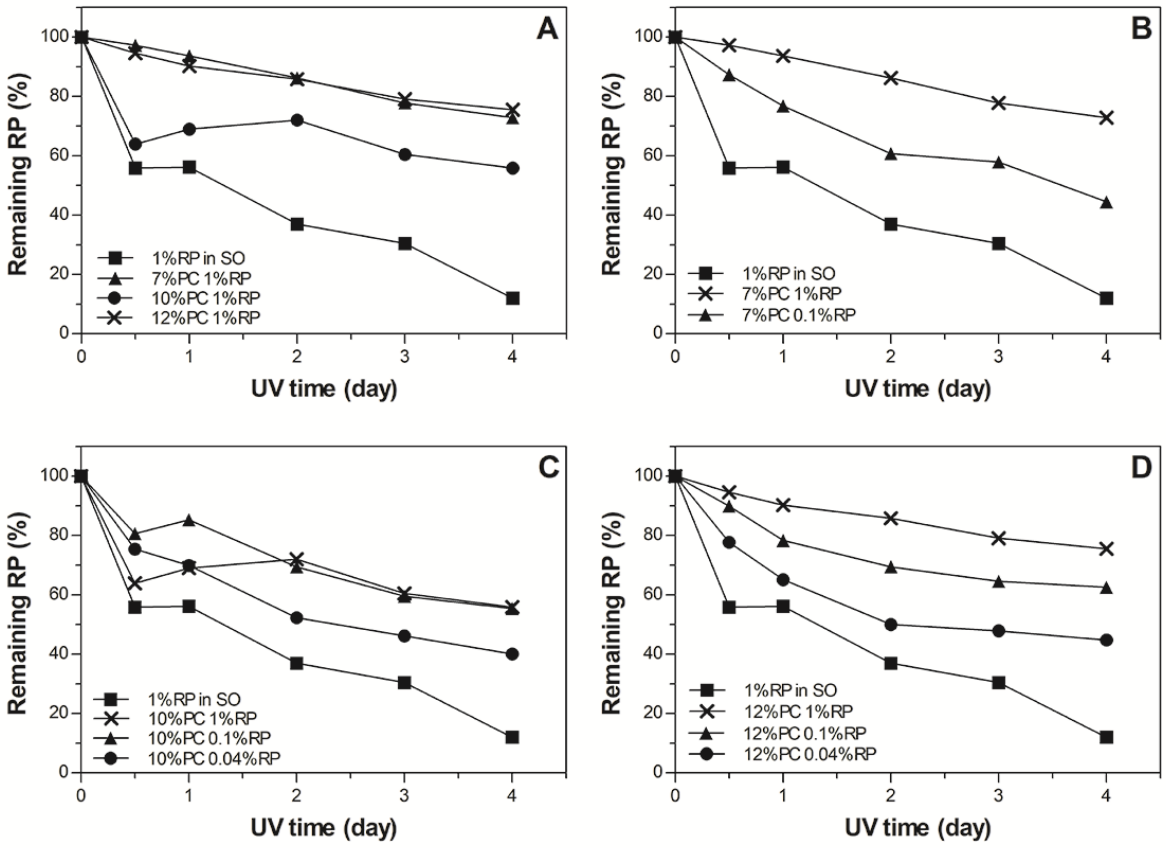

Figure 2.7 Remaining RP (%) values in (A) 1% RP in soybean oil and 7 - 12% (w/w) PCOs (B) 7%, (C) 10%, and (D) 12% (w/w) PCOs with 0.04%, 0.1%, and 1% RP (w/w) after different times (0, 0.5, 1, 2, 3, 4 days) of UVA radiation. 1% RP in soybean oil is shown in the figure as control.

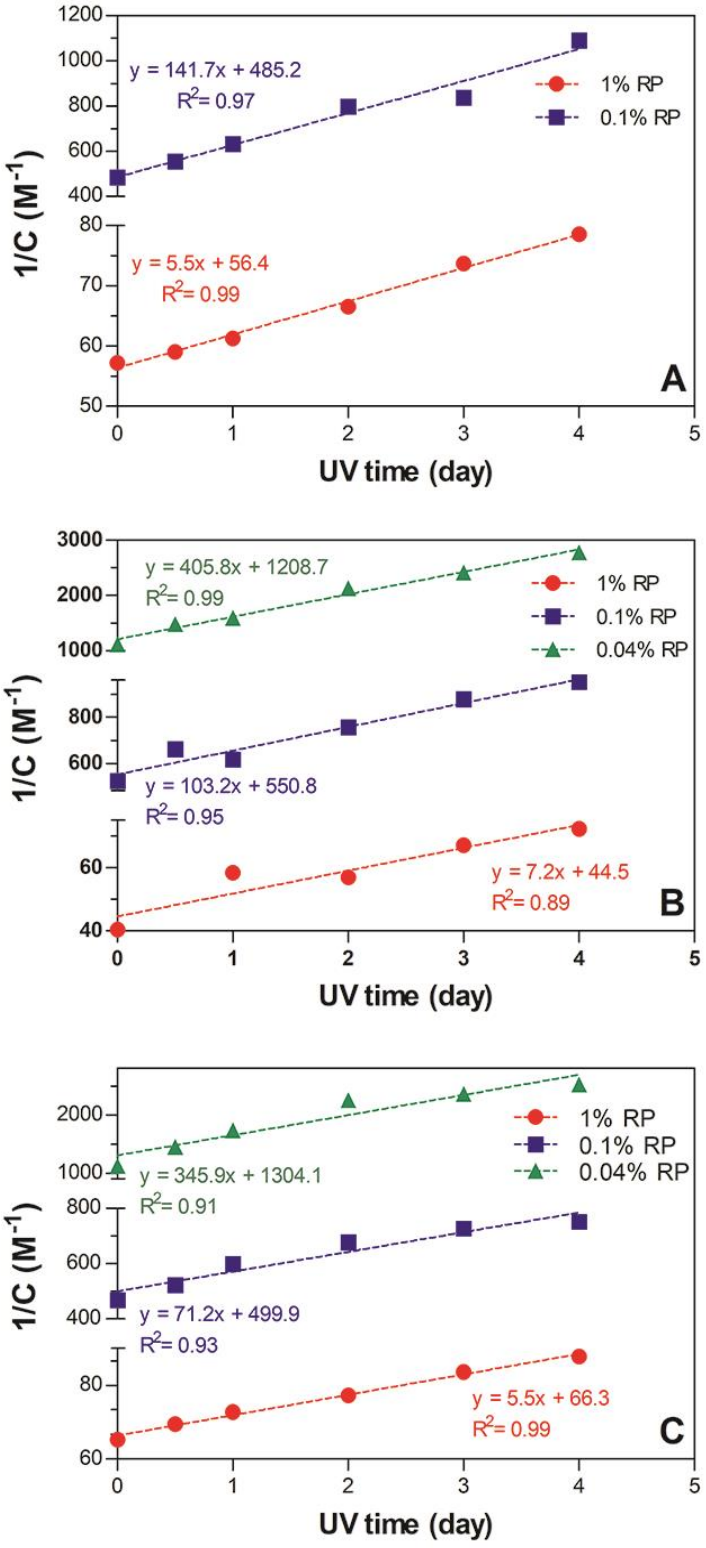

Figure 2.8 Inverse concentration of RP (M^{-1}) vs. UVA irradiation time: (A) 7%, (B) 10%, and (C) 12% PCOs (w/w)

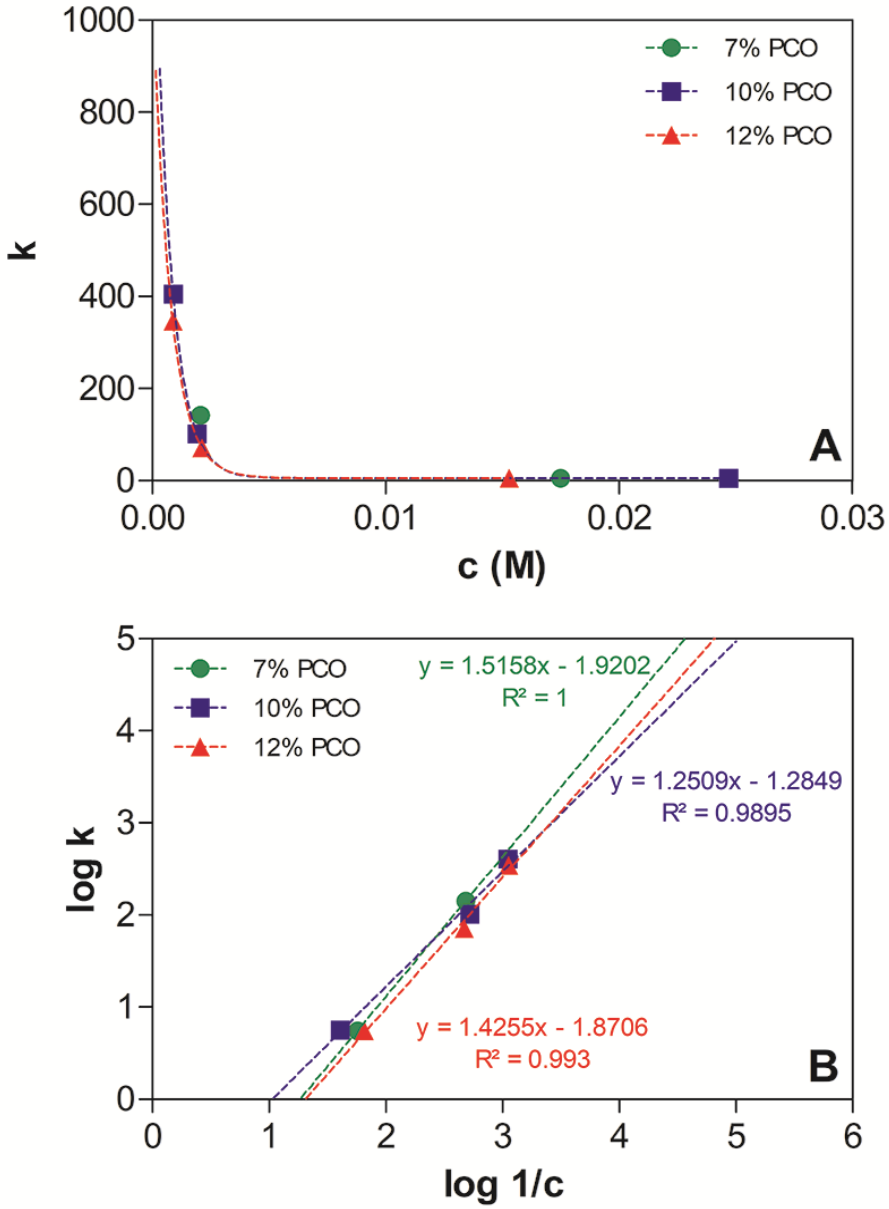

Figure 2.9 (A) Kinetic rate constants (k) vs. initial concentration of RP (B) Log_{10} of kinetic constants against log_{10} of the inverse initial concentration of RP

CHAPTER 3. PHOTOPROTECTIVE MECHANISM OF SUPRAMOLECULAR OLEOGELS ON RETINYL PALMITATE

A paper to be submitted to *Food Research International*

Yixing Tian[1,2] and Nuria C. Acevedo[1*]

Abstract

Exposure to ultraviolet radiation may cause significant degradation of retinyl palmitate (RP) leading to the loss of its biological activity. The objective of this study was to explore the protective mechanism of RP taking place in policosanol oleogels (PCOs); particularly, UV-barrier matrix effect, molecular immobilization and free radical-mediated reaction were studied. UV-blocking action was tested by placing a layer of 7% PCO (w/w) as barrier between UVA (365 nm) source and 1% RP in soybean oil. Structural effect on RP photostability was studied by cooling 7% and 12% PCOs with 1% RP (w/w) at different rates. The remaining % RP was measured by HPLC after 0 to 4 days of irradiation. PCOs microstructure and RP location in the network were studied by polarized light and fluorescence microscope. Matrix mobility was studied by low resolution NMR. Oil binding capacity was gravimetrically determined over short time storage. Peroxide values (PV) and p-anisidine values (p-A.V.) of 7% PCOs were determined up to 35 days of storage at 40˚C. It was found that PCOs can efficiently bock UVA energy absorption and further dampen the UVA mediated degradation. PCOs prepared at higher cooling rates had smaller crystal particle area sizes and provided better RP protection due to molecular immobilization.

[1] Department of Food Science and Human Nutrition, Iowa State University, Ames, IA 50011
[2] Primary researcher and author
[*] Author for correspondence

Microscopies and matrix mobility results suggested that PCOs efficiently immobilized RP in the network and improved RP photostability by reducing molecular collision. PV and p-A.V. results indicated that PCOs can improve oil oxidative stability and hinder the progress of radical-mediated oxidative reactions. In conclusion, the protective mechanism of RP in PCOs is a combined effect of physical UV-barrier action, molecular immobilization and inhibition of the free radical-mediated reaction.

Introduction

Vitamin A is an essential nutrient for human that plays an important role in visual functions, reproduction, cell growth and maintenance (Tee & Lee, 1992). Retinyl Palmitate (RP), the ester form of Vitamin A, is widely used in many products, including foods, drugs and cosmetics, because retinyl esters are more chemically and thermally stable than retinol (Ji & SEO, 1999). Retinoids have limited chemical and photochemical stability, that is strongly affected by environmental factors, including solvent, temperature and availability of oxygen (Deritter, 1982; Ji & SEO, 1999).

Several studies have been carried out on the chemical decomposition pathways of retinol and its esters, including thermal isomerization, dehydration and oxidation (Manan, Baines, Stone, & Ryley, 1995; McBee, et al., 2000; Różanowska, Cantrell, Edge, Land, Sarna, & Truscott, 2005; Tolleson, et al., 2005). It has been reported that esterification induced retinol to be more labile to photolysis (Ihara, Hashizume, Hirase, & SUZUE, 1999). UV irradiation can photoexcite retinol and its esters (Fu, et al., 2007) and mediate photoreactions, including isomerization, degradation, and oxidation (Crank & Pardijanto, 1995; Magdeleine Mousseron-Canet, 1971; M Mousseron-Canet, Mani, Favie, & Lerner, 1966; Tsujimoto, Hozoji, Ohashi, Watanabe, & Hattori, 1984; Xia, et al., 2006).

Based on the known mechanism of RP photoreaction, several strategies have been explored to improve photostability of RP. The entrapment or encapsulation of vitamin A has been used as a strategy to improve chemical and photochemical stability in different systems, such as emulsions (Carlotti, Rossatto, & Gallarate, 2002), hydrogels (Carlotti, Rossatto, Gallarate, Trotta, & Debernardi, 2004), solid lipid nanoparticles (Carlotti, Sapino, Trotta, Battaglia, Vione, & Pelizzetti, 2005; Jenning & Gohla, 2001), polymer encapsulation (Duclairoir, Irache, Nakache, Orecchioni, Chabenat, & Popineau, 1999; Çirpanli, ünlü, Çaliş, & Atilla Hincal, 2005). Addition of antioxidants has also been used as an approach to protect vitamin A from photooxidaiton (Carlotti, Rossatto, & Gallarate, 2002; Carlotti, Rossatto, Gallarate, Trotta, & Debernardi, 2004).

The chemical stability of RP in emulsion system was reported to be associated to the physical stability of emulsion and the presence of a coherent gel-like structure in the system (Semenzato, Bau, Dall'Aglio, Nicolini, Bettero, & Calliari, 1994). Solid lipid nanoparticles were found to provide physical UV-blocking action to protect RP from photoreactions (Carlotti, Sapino, Trotta, Battaglia, Vione, & Pelizzetti, 2005). In a previous study on self-assembled supramolecular gels, Wang, Fang, Li, Fu and Yang (2012) stated that RP molecules were isolated in the chambers of three-dimensional network structure and RP photostability was increased by reducing the molecular collisions and the degradation process of RP. It was found that encapsulated systems protected RP from hydrolysis and oxidation overtime, and improved the RP photostability (Carlotti, Rossatto, Gallarate, Trotta, & Debernardi, 2004). The aforementioned authors also stated that the presence of an antioxidant improved the photostability of RP, which suggested that oxygen was a photodegradation partner.

Oleogels are solid-like gel systems where the liquid phase is oil (Marangoni & Garti, 2011). Many studies have been performed on the encapsulation and delivery of bioactive compounds in oleogels, such as monoglyceride oleogel (Yu, Shi, Liu, & Huang, 2012), sorbitan monostearate oleogel (Murdan, Andrýsek, & Son, 2005), and 12-hydroxystearic acid oleogel (Iwanaga, Sumizawa, Miyazaki, & Kakemi, 2010). Sullivan et al. (2017) reported that ethylcellulose oleogels can improve oxidative stability of oil and a bioactive compound entrapped in the system. Similarly, in a previous study on policosanol oleogel (PCO), it was found that PCO can efficiently improve the photostability of RP entrapped in the oleogel system (Tian and Acevedo, 2017). However, the mechanism of RP protection taking place in PCO is not clear.

The overall goal of this study is to investigate the mechanism of RP protection in PCO system. Due to the similar system structure with solid lipid nanoparticles and self-assembled supramolecular gels, we hypothesize that PCOs can act as a physical UV-barrier, provide immobilization of RP in the system and delay free radical mediated reaction.

The study was designed to evaluate RP protection from three aspects: the physical UV-blocking action, the effect of oleogel structure, and the delay or hindering of free radical mediated reaction. Based on the results obtained in our previous study, 7% PCO (w/w) was chosen as matrix to study the mechanism of RP protection due to its higher efficiency to protect RP activity and low gelator concentration. 12% PCOs were selected as systems to study the effect of oleogel structure due their more developed crystalline network (Tian and Acevedo, 2017).

To test the physical UV-blocking action, 7% PCO (w/w) was placed on the top of RP in soybean (SO) as a barrier under UVA (365 nm) irradiation to compare with 1% RP

incorporated in 7% PCO. The % reaming all-*trans* RP was measured by high performance liquid chromatography (HPLC) after irradiation. The effect of PCOs structure on RP photostability was studied by preparing 7% and 12% PCOs with 1% RP (w/w) at different cooling rates. The % remaining RP in samples were measured after UVA irradiation. Remaining of RP after UVA irradiation, microstructure of PCOs, location of RP in the system, matrix mobility, and oil binding capacity were analyzed to study the effect PCOs structure on RP protection. Peroxide values (PV) and p-anisidine values (p-A.V.) were measured to determine the oxidative stability of 7% PCOs over storage time.

Martials and methods

Materials

Soybean oil was generously provided by ADM oils (Decatur, IL, USA). 98% Policosanol containing 60% octacosanol was purchased from PureBulk Inc. (Roseburg, OR, USA). RP (1,600,000 – 1,800,000 USP units per gram) and 2-Propanol (HPLC grade) were purchased from Sigma-Aldrich (St. Louis, MO, USA). Hexane (HPLC grade), ethyl ether, isooctane, glacial acetic acid, potassium iodide, sodium thiosulfate were from Fisher Chemical (Fair Lawn, NJ, USA). p-Anisidine (99%) was purchased from ACROS Organics (New Jersey, USA).

A UVA lamp Model ENF-280C (365 nm, 115V, 60Hz, 0.20 A) was used for UV treatment (Spectroline, NY, USA). The lamp provides 1.488×10^{-6} W/cm^2 measured by UV safety meter model 6D (Solar Light, Glenside, PA, USA).

Oleogel preparation

Policosanol (7 and 12%, w/w) was added to soybean oil. The samples were heated at 85 °C and stirred at 250 rpm for 30 minutes. RP (1%, w/w) was added and slightly mixed

after stirring. Samples were poured into plastic petri dishes (35 mm diameter and 4 mm height), afterward 7% PCOs were cooled at 2, 8, 25 °C/min and 12% PCOs were cooled at 8, 14, 25 °C/min. Samples were stored at 4 °C for one week before UVA treatment. SO with 1% RP was prepared with same method and used as control. The dishes were placed under the UVA lamp (365 nm) at 10 cm distance. Samples were irradiated for 0, 0.5, 1, 2, 3, and 4 days.

Analysis of UVA screening

7% PCOs and SO with 1% (w/w) RP were prepared as explained previously with a cooling rate of 8 °C/min. The 7% PCO dish was placed on the top of RP-SO dish, under the UVA lamp (325 nm) at 10 cm distance. RP-SO samples with empty petri dish on the top were used as controls in order to eliminate the blockage effect of petri dish. 1% RP in 7% PCO was placed under the UVA lamp. The setup of the experiment is shown in Figure **3.1**. Samples were irradiated for 0, 0.5, 1, 2, 3, and 4 days.

RP determination by HPLC

After UVA irradiation, samples were analyzed by high performance liquid chromatography (HPLC). Samples were transferred to HPLC amber vials and diluted with hexane to a RP concentration range from 0.01 to 0.1 mg/mL. At least three replicates of each samples were analyzed.

A method developed by Scalzo, Santucci, Cerreto, and Carafa (2004) with modifications was used to determine the residual concentration of *trans*-RP after UVA treatment by using normal phase HPLC. The HPCL instrument (Agilent 1100 Series LC/MSD Ion Trap; Santa Clara, CA, USA) was equipped with a diode array detector (DAD) G1315B (Agilent, Santa Clara, CA, USA). Analyses were carried out with a 50 mm × 4.6

mm SUPELCOSIL™ LC-Si (5µm) column (Sigma-Aldrich, St. Louis, MO, USA). Mobile phase A hexane: isopropanol (99:1, v/v) and mobile phase B ethyl ether was used as mobile phase solvent. The amount of ethyl ether was increased from 0 to 5% (v/v) over 5 mins and then decreased to 0% during the following 2 mins. The flow rate was 1 mL/min and the sample injection volume was 10 µL. The detector was set at 325 nm and the reference wavelength was 360 nm.

The HPLC chromatogram was integrated by Quant analysis for 6300Series Ion Trap LC/MS version 1.8 (Agilent, Santa Clara, CA, USA). The remaining RP (%) was calculated by using the following equation:

$$\text{Remaining RP (\%)} = \frac{\text{peak area of RP (Xd UV)}}{\text{peak area of RP (0d UV)}} \times 100\% \quad (1)$$

Microstructure

Differential interference contrast (DIC) microscopy was used to analyze the microstructure of the PCO samples. A small drop of liquid sample was placed between a preheated microscope slide and glass cover. The slides were subjected to a heating and cooling program by using cooling stage to achieve the desired cooling rate before observation. The images were acquired with a DIC microscope (Olympus BX53, Olympus Corporation, MA, USA) using the CellSens Dimension software (Olympus Corporation, MA, USA). Three replicates were prepared and 10 images of each slide were recorded. The images were analyzed by using software ImageJ (NIH, MD, USA) to report crystal particle area.

A fluorescence microscope was used to visualize the location of RP in SO and 7% PCOs since RP is fluorescent-active. The images were acquired with a fluorescence microscope (Zeiss Axio Imager Z2, Zeiss, Oberkochen, Germany) using the Zen Pro

software (Zeiss, Oberkochen, Germany). Three replicates were prepared and 10 images of each slide were recorded.

Oil binding capacity

To test the oil binding capacity of PCO samples, discs were prepared by pouring the hot liquid oleogel mixture into PVC disc molds (22 mm diameter and 3.2 mm thickness). 7% PCOs were cooled in the molds at 2, 8, 25 C/min and 12% PCOs were cooled at 8, 14, 25 C/min. Samples were stored at that 4 °C for a week before analysis. Each oleogel disc was removed from the mold, placed on a round filter paper (Whatman #5, 110 mm diameter) and incubated at 20 °C. The weight of each filter paper was recorded after 0, 24, and 48 hours of storage time. A filter paper without sample on it was used as control in the experiments to account for the environment effect on the filter papers. Filter papers were large enough to absorb all the oil released from samples during the experiment without saturation. At least 10 replicates were prepared and means and standard deviations are reported. Oil loss (%) was calculated by using the following equation:

$$\% \text{ Oil Loss} = \frac{[wt.paper\ (x\ h) - wt.paper\ (0\ h)] - [wt.blank\ (x\ h) - wt.blank\ (0\ h)]}{Total\ mass\ of\ sample} \times 100 \qquad (2)$$

Matrix molecular mobility

Matrix mobility of PCOs were measured by ^{1}H nuclear magnetic resonance (NRM) spectrometery (Bruker Bio Spin Corporation, Billercia, MA, USA). Liquid PCO samples were poured into flat-bottom glass NMR tube (10 mm diameter, 180 mm length) up to a height of 1 cm and cooled at cooling rate ranging 2 to 25 °C/min and afterwards stored at 4 °C for one week before testing. Each sample was prepared and analyzed in triplicate; means and standard deviations are reported.

The Carr-Purcell-Meiboom-Gill (CPMG) pulse sequence was used to measure spin-spin relaxation time (T_2) values between 0 and 1000 millisecond (ms). The separation between the 90° and 180° pulse was 0.04 tau and 4000 data points were collected. A total of 32 scans were run with a 1.5 s recycle delay and gain of 58 dB. Relaxation curves were fitted to a continuous distribution of exponentials using the CONTIN algorithm (Bruker software, Bruker BioSpin Corporation, Billerica, MA).

Analysis of oxidative stability

SO and 7% PCO samples with 1% RP were prepared to study the oxidation stability. Hot SO and 7% PCO samples were poured into flat-bottom glass vials (2 cm diameter, 8.5 cm length) up to a height of 4 cm and cooled at 8 °C/min. After storage at 4 °C for one week, samples were incubated at 40 °C for 35 days. PV and p-A.V. were measured at 0, 3, 5, 15, 25, and 35 days using AOCS Official Method (*AOCS Aocs official method cd 8b-90.*, 2011). Each sample was analyzed in triplicate; means and standard deviations are reported.

Statistical analysis

Statistical analysis was carried out with Graph Pad Prism 5 (GraphPad Software, Inc., La Jolla, CA, USA). One-way analysis of variance (ANOVA) tests were conducted with Tukey's post test to adjust multiple comparisons. Significant differences were defined as p-value < 0.05.

Results and Discussion

Analysis of UVA screening

7% PCO was placed on the top of 1% RP-SO sample as to asses if PCO can provide physical UV-blocking action to protect RP against UVA-mediated degradation. The

remaining % RP in samples after UVA irradiation are shown in Figure **3.2**. It can be observed that 7% PCO can efficiently protect 1% RP-SO from photodegradation, which suggests that PCOs can block the energy absorption from UVA irradiation. The 7% PCO placed on the top served as a barrier and protected over 89% of RP in RP-SO after 4 days of UVA irradiation, which is 16% higher than that remaining % RP in RP-PCO samples. This difference is perhaps due to the low UV-blocking action for the RP that is dispersed on the surface of PCO matrices. After 4 days of irradiation, RP-SO lost over 47% of RP, while it only lost 11% of RP when PCO was placed on the top. These results indicate that PCO matrices can block the energy absorption from UVA irradiation and protect RP from UVA-mediated degradation. This effect is probably associated to the crystalline network present in PCO matrices. Crystal particle area size in 7% PCO were reported to be $148.3 \pm 2.7\ \mu m^2$ (Tian and Acevedo, 2017), which is significantly higher than the wavelength of UVA source (365 nm) used in this experiment. Thus, 7% PCO provides an effective UVA obstruction to improve the photostability of RP.

These results are in line with previous studies on RP stability. It was reported that the chemical stability of RP depended on the physical stability and the presence of a coherent gel-like structure in emulsion system (Semenzato, Bau, Dall'Aglio, Nicolini, Bettero, & Calliari, 1994). It was found that solid lipid nanoparticles improved RP photostability over time through physical UV-blocking action (Carlotti, Sapino, Trotta, Battaglia, Vione, & Pelizzetti, 2005).

Microstructure

Microstructural properties of 7% and 12% PCOs prepared at different cooling rates were studied to establish the relationship between RP protection and crystalline network

characteristics. Typical microscopy images of PCOs are shown in Figure **3.3**. 7% PCOs microstructures are characterized by large, needle-like crystals. At low PC concentration, large crystals were formed and distributed far from another in the matrix without much interaction. As expected, with the increase in cooling rate, the crystal particle area (166.4 ± 14.6 μm^2 at 2 °C/min, 148.3 ± 2.7 μm^2 at 8 °C/min, and 60.9 ± 5.2 μm^2 at 25 °C/min) decreased. Faster cooling rate associates with a higher time-dependent undercooling or supersaturation, which leads to faster rate of nucleation resulting in a higher population of small crystals (Rogers & Marangoni, 2008). Similar results were found in sunflower wax oleogels that rapid cooling decreased the crystal length and network pore area fraction (Blake & Marangoni, 2014). The same trend was found in 12% PCOs prepared at different cooling rates (55.0 ± 3.5 μm^2 at 8 °C/min, 43.0 ± 1.8 μm^2 at 14 °C/min, and 26.9 ± 0.6 μm^2 at 25 °C/min). In 12% PCOs, higher concentration of PC in the matrix promoted the growth and expansion of the crystalline structure due to the higher supersaturation, which resulted in the formation of dense and big crystalline aggregates. These results suggest that preparation cooling rate has a significant impact on the network structure formed in PCOs.

Typical fluorescence microscopy images of SO and 7% PCOs with and without RP are shown in Figure **3.4**. Almost no luminescence can be observed in SO (Figure **3.4** A) and SO containing RP (Figure **3.4** B), which indicates that RP is homogeneously dispersed in liquid SO. Compared with 7% PCO (Figure **3.4** C), RP-PCO (Figure **3.4** D) shows significantly enhanced luminescence, especially in the boundaries of the crystalline network. These results suggest that the crystalline network structure can immobilize RP in PCO matrix, which would be related to the improvement of RP photostability by reducing molecular collisions (Semenzato, Bau, Dall'Aglio, Nicolini, Bettero, & Calliari, 1994).

Similar results were reported by Wang, Fang, Li, Fu, and Yang (2012). The mentioned authors found that self-assembled supramolecular gels isolated RP in the "chambers" of three-dimensional networks, which protected RP from photodegradation. Similarly, it was found that ethylcellulose oleogels protected beta-carotene, which was located in the connected pockets within polymer network, through reducing the diffusion of beta-carotene (Sullivan, Davidovich-Pinhas, Wright, Barbut, & Marangoni, 2017).

Oil binding capacity

Oil binding capacity of PCO samples prepared at different cooling rate was analyzed through oil loss values (% OL) in order to determine the PCO stability during short time storage. % OL values obtained from all the PCO samples as a function of time are shown in Figure **3.5**. As expected, 7% PCO prepared at low cooling rate showed the highest % OL due to the bigger crystals and weak network formed. This frail network was not able to entrap liquid oil effectively, which led to OL values of 16.9 ± 1.4% and 24.2 ± 1.8% after 24 and 48 hours of storage, respectively. These results are in line with those of Dibildox-Alvarado, Rodrigues, Gioielli, Toro-Vazquez and Marangoni's (2004). The authors reported that larger crystals led to a greater oil loss, where crystal size was varied by crystallization of fat at different cooling rate. Surprisingly, there is no significant difference ($p < 0.05$) found between 7% PCOs prepared at 8 and 25 °C/min. As shown in the microscopy images (Figure **3.3**), smaller crystals were formed in 7% PCO prepared at 25 °C/min than that prepared at 8 °C/min. However, it didn't influence the oil binding capacity significantly perhaps due to the low PC concentration in the system.

With higher PC concentration in matrix, 12% PCOs have significantly lower % OL values than 7% PCOs, which is associated with the smaller crystal particle area (Figure **3.3**)

and a stronger network formed in 12% PCOs. When preparation cooling rate was raised from 8 to 14 °C/min, the %OL values of 12% PCOs significantly decreased due to the decrease of crystal particle area in matrix. However, the %OL values of 12% PCOs was significantly higher at a cooling rate of 25 °C/min. As a previous study stated (Tian and Acevedo, 2017), 12% PCOs takes longer time to create a stable crystal network. At a high cooling rate (25 °C/min), 12% PCOs is not able to create a stable network and entrap liquid oil efficiently during the short cooling stage. When the short time storage oil loss test was conducted, it released these part of oil that not entrapped in the network.

Effect of cooling rate on RP photostability

The % remaining RP in 7% and 12% PCOs prepared at different cooling rates are shown in Figure **3.6**. For 1% RP in 7% PCOs prepared at different cooling rates, no significant difference ($p < 0.05$) in the RP protection can be observed. Even though a different microstructure was resulted from cooling at different rates, perhaps, crystal size differences are not determining protection in this network where a lower PC concentration is present. Overall, there is a high RP protection efficiency in all 7% PCO samples. For 12% PCO, there is a trend of improvement in the RP protection at fast cooling rates. The small crystal particle area size and stronger network formed in 12% PCOs prepared at higher cooling rats can block energy absorption more efficiently and provide better immobilization of RP. Even though there is a trend where higher cooling rates lead to higher RP protection, particularly at 12% PCO, matrices prepared at different cooling rate did not show significant difference on RP protection.

Matrix molecular mobility

The respective spin-spin relaxation times (T_2) spectra of SO and PCOs prepared at different cooling rates are shown in Figure **3.7**. It was found that SO had a significant ($p < 0.05$) higher T_2 than PCOs regardless of the PC ratio and preparation cooling rate, which indicates that PCOs immobilized matrix molecular in the networks. These results support the previous finds from florescence microscopy that PCOs network immobilized RP in the system and further reduced RP degradation. There is a trend where PCOs prepared that at a high cooling rate have a lower T_2 value than that prepared at low cooling rate, which is associated with a lower molecular mobility. These results suggest that PCOs prepared at higher cooling rates led to better immobilization and more efficient protection of RP.

Analysis of oxidative stability

Free radical-mediated reaction is involved in the UVA mediated RP degradation. Crank and Pardijanto (1995) found that singlet oxygen initiated the photooxidation of RP and produced anhydroretinol and fragments derived from cleavage of the side-chain double bonds. It was found that vitamin A in highly peroxidized soybean oil (PV > 10 mequiv O_2/kg) decreased in a doubling rate when exposed to fluorescent light compared to vitamin A in mildly oxidized oil (PV < 2 mequiv O_2/kg) (Pignitter, Dumhart, Gartner, Jirsa, Steiger, Kraemer, et al., 2014). These authors pointed out that the oxidative status of the oil used for RP fortification has an impact on the stability of RP. PV is a common parameter used to characterize the oxidative state of oil and p-A.V. indicates the amount of secondary oxidation products (Steele, 2004).

In order to investigate the oxidative stability of oil in PCOs and whether PCOs can delay free radical mediated reaction, PV and p-A.V. were measured overtime (Figure **3.8**). It

was found that SO samples have higher PV and p-A.V. than 7% PCOs over time and the differences became significant ($p < 0.05$) after 25 days of storage. After 35 days, the PV of SO is 34.3 ± 6.5 meq O_2/kg, while PV of 7% PCO is 16.8 ± 0.8 meq O_2/kg. The high oil oxidative stability in PCOs is beneficial to improve the photostability of RP in the system based on previous study (Pignitter, et al., 2014). Compared with liquid soybean oil, PCOs can prevent the free radical-mediated photooxidation of RP. Similar results were reported by Sullivan, Davidovich-Pinhas, Wright, Barbut, and Marangoni (2017) that ethylcellulose oleogels protected beta-carotene from oxidation at high temperature, which was related to the reducing of beta-carotene diffusion. These results suggest that PCOs can improve oil oxidative stability and effectively hinder the progress of radical-mediated oxidative reactions.

Conclusion

This study focused on the mechanism of RP protection in PCOs. From the UVA blockage study, it was found that PCOs can efficiently block UVA energy absorption and further protect RP from UVA mediated photodegradation. Preparation cooling rate has a significant impact on the network structure formed in PCOs. 7% and 12% (w/w) PCOs prepared at higher cooling rates had smaller crystal particle area sizes and provided better RP protection due to the molecular immobilization. The florescence microscopy and low resolution NMR results supported that PCOs immobilized RP in the network and reduced molecular collision. PV and p-A.V. of SO and 7% PCOs showed that PCOs can effectively hinder the progress of radical-mediated oxidative reactions. The mechanism of RP protection in PCOs includes the physical UVA blocking action, the immobilization of RP in the system and inhibition of the free radical-mediated reaction. Future study should focus on the *in vitro*

bioaccessibility of RP in PCOs to investigate the properties of PCOs as an oral delivery system.

Reference

Abdallah, D. J., Lu, L., & Weiss, R. G. (1999). Thermoreversible organogels from alkane gelators with one heteroatom. Chemistry of materials, 11(10), 2907-2911.

Acevedo, N. C., Block, J. M., & Marangoni, A. G. (2012). Critical laminar shear-temperature effects on the nano-and mesoscale structure of a model fat and its relationship to oil binding and rheological properties. Faraday discussions, 158(1), 171-194.

Aguilera, J., Michel, M., & Mayor, G. (2004). Fat migration in chocolate: diffusion or capillary flow in a particulate solid?—a hypothesis paper. Journal of Food Science, 69(7), 167-174.

Allwood, M., & Plane, J. (1986). The wavelength-dependent degradation of vitamin A exposed to ultraviolet radiation. International journal of pharmaceutics, 31(1-2), 1-7.

Almeida, I. F., & Bahia, M. F. (2006). Evaluation of the physical stability of two oleogels. International journal of pharmaceutics, 327(1), 73-77.

AOCS Aocs official method cd 8b-90. (2011).

Avramiotis, S., Papadimitriou, V., Hatzara, E., Bekiari, V., Lianos, P., & Xenakis, A. (2007). Lecithin organogels used as bioactive compounds carriers. A microdomain properties investigation. Langmuir, 23(8), 4438-4447.

Ball, G. (1998). Vitamin A and the provitamin A carotenoids. In Bioavailability and Analysis of Vitamins in Foods, (pp. 115-161): Springer.

Biesalski, H. K., & Nohr, D. (2004). New aspects in vitamin A metabolism: the role of retinyl esters as systemic and local sources for retinol in mucous epithelia. The Journal of nutrition, 134(12), 3453S-3457S.

Blake, A. I., & Marangoni, A. G. (2014). Structure and physical properties of plant wax crystal networks and their relationship to oil binding capacity. Journal of the American Oil Chemists' Society, 91(6), 885-903.

Carafa, M., Marianecci, C., Salvatorelli, M., Di Marzio, L., Cerreto, F., Lucania, G., & Santucci, E. (2008). Formulations of retinyl palmitate included in solid lipid nanoparticles: characterization and influence on light-induced vitamin degradation. Journal of Drug Delivery Science and Technology, 18(2), 119-124.

Carlotti, M., Rossatto, V., & Gallarate, M. (2002). Vitamin A and vitamin A palmitate stability over time and under UVA and UVB radiation. International journal of pharmaceutics, 240(1), 85-94.

Carlotti, M., Rossatto, V., Gallarate, M., Trotta, M., & Debernardi, F. (2004). Vitamin A palmitate photostability and stability over time. International Journal of Cosmetic Science, 26(5), 270-270.

Carlotti, M., Sapino, S., Trotta, M., Battaglia, L., Vione, D., & Pelizzetti, E. (2005). Photostability and stability over time of retinyl palmitate in an O/W emulsion and in SLN introduced in the emulsion. Journal of dispersion science and technology, 26(2), 125-138.

Cherng, S.-H., Xia, Q., Blankenship, L. R., Freeman, J. P., Wamer, W. G., Howard, P. C., & Fu, P. P. (2005). Photodecomposition of retinyl palmitate in ethanol by UVA light

formation of photodecomposition products, reactive oxygen species, and lipid peroxides. Chemical research in toxicology, 18(2), 129-138.
Coates, P. M., Blackman, M. R., Cragg, G. M., Levine, M., Moss, J., & White, J. D. (2004). Encyclopedia of dietary supplements: CRC Press.
Crank, G., & Pardijanto, M. S. (1995). Photo-oxidations and photosensitized oxidations of vitamin A and its palmitate ester. Journal of Photochemistry and Photobiology A: Chemistry, 85(1-2), 93-100.
Da Pieve, S., Calligaris, S., Nicoli, M. C., & Marangoni, A. G. (2010). Shear nanostructuring of monoglyceride organogels. Food Biophysics, 5(3), 211-217.
Daniel, J., & Rajasekharan, R. (2003). Organogelation of plant oils and hydrocarbons by long-chain saturated FA, fatty alcohols, wax esters, and dicarboxylic acids. Journal of the American Oil Chemists' Society, 80(5), 417-421.
Dassanayake, L. S. K., Kodali, D. R., & Ueno, S. (2011). Formation of oleogels based on edible lipid materials. Current opinion in colloid & interface science, 16(5), 432-439.
Deritter, E. (1982). Vitamins in pharmaceutical formulations. Journal of pharmaceutical sciences, 71(10), 1073-1096.
Dibildox-Alvarado, E., Rodrigues, J. N., Gioielli, L. A., Toro-Vazquez, J. F., & Marangoni, A. G. (2004). Effects of crystalline microstructure on oil migration in a semisolid fat matrix. Crystal growth & design, 4(4), 731-736.
Duclairoir, C., Irache, J. M., Nakache, E., Orecchioni, A. M., Chabenat, C., & Popineau, Y. (1999). Gliadin nanoparticles: formation, all-trans-retinoic acid entrapment and release, size optimization. Polymer international, 48(4), 327-333.
Dunford, N. T., Irmak, S., & Jonnala, R. (2010). Pressurised solvent extraction of policosanol from wheat straw, germ and bran. Food chemistry, 119(3), 1246-1249.
Final Determination Regarding Partially Hydrogenated Oils (Removing Trans Fat). In. (2015), vol. 2017): U.S. Food and Drug Administration.
Flanagan, J., & Singh, H. (2006). Microemulsions: a potential delivery system for bioactives in food. Critical reviews in food science and nutrition, 46(3), 221-237.
Fu, P. P., Xia, Q., Yin, J. J., Cherng, S. H., Yan, J., Mei, N., Chen, T., Boudreau, M. D., Howard, P. C., & Wamer, W. G. (2007). Photodecomposition of vitamin A and photobiological implications for the skin. Photochemistry and photobiology, 83(2), 409-424.
Gandolfo, F. G., Bot, A., & Flöter, E. (2004). Structuring of edible oils by long-chain FA, fatty alcohols, and their mixtures. Journal of the American Oil Chemists' Society, 81(1), 1-6.
Gouni-Berthold, I., & Berthold, H. K. (2002). Policosanol: clinical pharmacology and therapeutic significance of a new lipid-lowering agent. American heart journal, 143(2), 356-365.
Gravelle, A., Davidovich-Pinhas, M., Zetzl, A., Barbut, S., & Marangoni, A. (2016). Influence of solvent quality on the mechanical strength of ethylcellulose oleogels. Carbohydrate polymers, 135, 169-179.
Ihara, H., Hashizume, N., Hirase, N., & SUZUE, R. (1999). Esterification makes retinol more labile to photyolysis. Journal of nutritional science and vitaminology, 45(3), 353-358.
Irmak, S., Dunford, N. T., & Milligan, J. (2006). Policosanol contents of beeswax, sugar cane and wheat extracts. Food Chemistry, 95(2), 312-318.

Iwanaga, K., Sumizawa, T., Miyazaki, M., & Kakemi, M. (2010). Characterization of organogel as a novel oral controlled release formulation for lipophilic compounds. International journal of pharmaceutics, 388(1), 123-128.

Jenning, V., & Gohla, S. H. (2001). Encapsulation of retinoids in solid lipid nanoparticles (SLN). Journal of microencapsulation, 18(2), 149-158.

Jeong, Y.-I., Song, J.-G., Kang, S.-S., Ryu, H.-H., Lee, Y.-H., Choi, C., Shin, B.-A., Kim, K.-K., Ahn, K.-Y., & Jung, S. (2003). Preparation of poly (DL-lactide-co-glycolide) microspheres encapsulating all-trans retinoic acid. International journal of pharmaceutics, 259(1), 79-91.

Ji, H.-G., & SEO, B.-S. (1999). Retinyl palmitate at 5% in a cream: its stability, efficacy and effect. Cosmetics and toiletries, 114(3), 61-68.

Jung, M., Lee, K., & Kim, S. (1998). Retinyl palmitate isomers in skim milk during light storage as affected by ascorbic acid. Journal of food science, 63(4), 597-600.

Kong, R., Xia, Q., & Liu, G. Y. (2011). Preparation and characterization of vitamin A palmitate-loaded nanostructured lipid carriers as delivery systems for food products. In Advanced Materials Research, vol. 236 (pp. 1818-1823): Trans Tech Publ.

Lim, S.-J., Lee, M.-K., & Kim, C.-K. (2004). Altered chemical and biological activities of all-trans retinoic acid incorporated in solid lipid nanoparticle powders. Journal of controlled release, 100(1), 53-61.

Loveday, S. M., & Singh, H. (2008). Recent advances in technologies for vitamin A protection in foods. Trends in food science & technology, 19(12), 657-668.

Lupi, F. R., Gabriele, D., Baldino, N., Mijovic, P., Parisi, O. I., & Puoci, F. (2013). Olive oil/policosanol organogels for nutraceutical and drug delivery purposes. Food & function, 4(10), 1512-1520.

Lupi, F. R., Gabriele, D., Greco, V., Baldino, N., Seta, L., & de Cindio, B. (2013). A rheological characterisation of an olive oil/fatty alcohols organogel. Food Research International, 51(2), 510-517.

Lupi, F. R., Gabriele, D., Seta, L., Baldino, N., & de Cindio, B. (2014). Rheological design of stabilized meat sauces for industrial uses. European Journal of Lipid Science and Technology, 116(12), 1734-1744.

Maiti, M., Roy, A., & Roy, S. (2014). Effect of pH and amphiphile concentration on the gel-emulsion of sodium salt of 2-dodecylpyridine-5-boronic acid: Entrapment and release of vitamin B 12. Colloids and Surfaces A: Physicochemical and Engineering Aspects, 461, 76-84.

Manan, F., Baines, A., Stone, J., & Ryley, J. (1995). The kinetics of the loss of all-trans retinol at low and intermediate water activity in air in the dark. Food Chemistry, 52(3), 267-273.

Marangoni, A. G. (2012). Organogels: an alternative edible oil-structuring method. Journal of the American Oil Chemists' Society, 89(5), 749-780.

Marangoni, A. G., & Garti, N. (2011). Edible oleogels: structure and health implications: Elsevier.

McBee, J. K., Kuksa, V., Alvarez, R., de Lera, A. R., Prezhdo, O., Haeseleer, F., Sokal, I., & Palczewski, K. (2000). Isomerization of all-trans-retinol to cis-retinols in bovine retinal pigment epithelial cells: dependence on the specificity of retinoid-binding proteins. Biochemistry, 39(37), 11370.

Micronutrients, I. o. M. P. o. (2001). Dietary Reference Intakes for Vitamin A, Vitamin K, Arsenic, Boron, Chromium, Copper, Iodine, Iron, Manganese, Molybdenum, Nickel, Silicon, Vanadium, and Zinc: National Academies Press (US).

Mousseron-Canet, M. (1971). [242] Photochemical transformation of vitamin A. Methods in enzymology, 18, 591-615.

Mousseron-Canet, M., Mani, J., Favie, C., & Lerner, D. (1966). On the photochemical isomerization of vitamin A. Compt. Rend, 262, 153-155.

Murdan, S., Andrýsek, T., & Son, D. (2005). Novel gels and their dispersions—oral drug delivery systems for ciclosporin. International journal of pharmaceutics, 300(1), 113-124.

Murphy, P. A., Engelhardt, R., & Smith, S. E. (1988). Isomerization of retinyl palmitate in fortified skim milk under retail fluorescent lighting. Journal of agricultural and food chemistry, 36(3), 592-595.

Ojijo, N. K., Neeman, I., Eger, S., & Shimoni, E. (2004). Effects of monoglyceride content, cooling rate and shear on the rheological properties of olive oil/monoglyceride gel networks. Journal of the Science of Food and Agriculture, 84(12), 1585-1593.

Omonov, T. S., Bouzidi, L., & Narine, S. S. (2010). Quantification of oil binding capacity of structuring fats: A novel method and its application. Chemistry and physics of lipids, 163(7), 728-740.

Pignitter, M., Dumhart, B., Gartner, S., Jirsa, F., Steiger, G., Kraemer, K., & Somoza, V. (2014). Vitamin A is rapidly degraded in retinyl palmitate-fortified soybean oil stored under household conditions. Journal of agricultural and food chemistry, 62(30), 7559-7566.

Pople, P. V., & Singh, K. K. (2006). Development and evaluation of topical formulation containing solid lipid nanoparticles of vitamin A. Aaps Pharmscitech, 7(4), E63-E69.

Raut, S., Bhadoriya, S. S., Uplanchiwar, V., Mishra, V., Gahane, A., & Jain, S. K. (2012). Lecithin organogel: A unique micellar system for the delivery of bioactive agents in the treatment of skin aging. Acta Pharmaceutica Sinica B, 2(1), 8-15.

Rogers, M. A., & Marangoni, A. G. (2008). Non-isothermal nucleation and crystallization of 12-hydroxystearic acid in vegetable oils. Crystal Growth and Design, 8(12), 4596-4601.

Rogers, M. A., Strober, T., Bot, A., Toro-Vazquez, J. F., Stortz, T., & Marangoni, A. G. (2014). Edible oleogels in molecular gastronomy. International Journal of Gastronomy and Food Science, 2(1), 22-31.

Rogers, M. A., Wright, A. J., & Marangoni, A. G. (2009). Nanostructuring fiber morphology and solvent inclusions in 12-hydroxystearic acid/canola oil organogels. Current opinion in colloid & interface science, 14(1), 33-42.

Różanowska, M., Cantrell, A., Edge, R., Land, E. J., Sarna, T., & Truscott, T. G. (2005). Pulse radiolysis study of the interaction of retinoids with peroxyl radicals. Free Radical Biology and Medicine, 39(10), 1399-1405.

Sane, A., & Limtrakul, J. (2009). Formation of retinyl palmitate-loaded poly (l-lactide) nanoparticles using rapid expansion of supercritical solutions into liquid solvents (RESOLV). The Journal of Supercritical Fluids, 51(2), 230-237.

Scalzo, M., Santucci, E., Cerreto, F., & Carafa, M. (2004). Model lipophilic formulations of retinyl palmitate: influence of conservative agents on light-induced degradation. Journal of pharmaceutical and biomedical analysis, 34(5), 921-931.

Schaink, H., Van Malssen, K., Morgado-Alves, S., Kalnin, D., & Van der Linden, E. (2007). Crystal network for edible oil organogels: possibilities and limitations of the fatty acid and fatty alcohol systems. Food Research International, 40(9), 1185-1193.

Semenzato, A., Bau, A., Dall'Aglio, C., Nicolini, M., Bettero, A., & Calliari, I. (1994). Stability of vitamin A palmitate in cosmetic emulsions: influence of physical parameters. International journal of cosmetic science, 16(4), 139-147.

Seo, S. H., & Chang, J. Y. (2005). Organogels from 1 H-Imidazole Amphiphiles: Entrapment of a Hydrophilic Drug into Strands of the Self-Assembled Amphiphiles. Chemistry of materials, 17(12), 3249-3254.

Sommer, A. (2008). Vitamin A deficiency and clinical disease: an historical overview. The Journal of nutrition, 138(10), 1835-1839.

Steele, R. (2004). Understanding and measuring the shelf-life of food: Woodhead Publishing.

Sullivan, C. M., Davidovich-Pinhas, M., Wright, A. J., Barbut, S., & Marangoni, A. G. (2017). Ethylcellulose oleogels for lipophilic bioactive delivery–effect of oleogelation on in vitro bioaccessibility and stability of beta-carotene. Food & Function, 8(4), 1438-1451.

Tanumihardjo, S. A. (2011). Vitamin A: biomarkers of nutrition for development. The American journal of clinical nutrition, 94(2), 658S-665S.

Tatariunas, A., & Matsumoto, S. (2000). A retinyl palmitate model of the phenomenon of the intrinsic fluorescence increase in ceroid-lipofuscin cytosomes. Experimental gerontology, 35(9), 1327-1341.

Tee, E. S., & Lee, C. (1992). Carotenoids and retinoids in human nutrition. Critical Reviews in Food Science & Nutrition, 31(1-2), 103-163.

Tokuyama, H., & Kato, Y. (2010). Preparation of thermosensitive polymeric organogels and their drug release behaviors. European Polymer Journal, 46(2), 277-282.

Tolleson, W. H., Cherng, S.-H., Xia, Q., Boudreau, M., Yin, J. J., Wamer, W. G., Howard, P. C., Yu, H., & Fu, P. P. (2005). Photodecomposition and phototoxicity of natural retinoids. International journal of environmental research and public health, 2(1), 147-155.

Toro-Vazquez, J., Morales-Rueda, J., Dibildox-Alvarado, E., Charó-Alonso, M., Alonzo-Macias, M., & González-Chávez, M. (2007). Thermal and textural properties of organogels developed by candelilla wax in safflower oil. Journal of the American Oil Chemists' Society, 84(11), 989-1000.

Tsujimoto, K., Hozoji, H., Ohashi, M., Watanabe, M., & Hattori, H. (1984). WAVELENGTH-DEPENDENT PEROXIDE FORMATION UPON IRRADIATION OF all-trans RETINAL IN AN AERATED SOLUTION. Chemistry Letters, 13(10), 1673-1676.

Varady, K. A., Wang, Y., & Jones, P. J. (2003). Role of policosanols in the prevention and treatment of cardiovascular disease. Nutrition reviews, 61(11), 376-383.

Vithanage, C. R., Grimson, M. J., & Smith, B. G. (2009). The effect of temperature on the rheology of butter, a spreadable blend and spreads. Journal of texture studies, 40(3), 346-369.

Wang, H., Fang, F., Li, X., Fu, C., & Yang, Y. (2012). Improved photostability of Vitamin A palmitate originating from self-assembled supramolecular gels. Chinese Science Bulletin, 57(33), 4257-4263.

Wohl, M. G., & Goodhart, R. S. (1960). Modern Nutrition in Health and Disease. Academic Medicine, 35(5), 463.
Xia, Q., Yin, J. J., Wamer, W. G., Cherng, S.-H., Boudreau, M. D., Howard, P. C., Yu, H., & Fu, P. P. (2006). Photoirradiation of retinyl palmitate in ethanol with ultraviolet light-formation of photodecomposition products, reactive oxygen species, and lipid peroxides. International journal of environmental research and public health, 3(2), 185-190.
Xu, Z., Fitz, E., Riediger, N., & Moghadasian, M. H. (2007). Dietary octacosanol reduces plasma triacylglycerol levels but not atherogenesis in apolipoprotein E–knockout mice. Nutrition research, 27(4), 212-217.
Yaghmur, A., De Campo, L., Sagalowicz, L., Leser, M., Glatter, O., Michel, M., & Watzke, H. J. (2012). Oil-in-water emulsion for delivery. In): Google Patents.
Yoshida, K., Sekine, T., Matsuzaki, F., Yanaki, T., & Yamaguchi, M. (1999). Stability of vitamin A in oil-in-water-in-oil-type multiple emulsions. Journal of the American Oil Chemists' Society, 76(2), 1-6.
Yu, H., Shi, K., Liu, D., & Huang, Q. (2012). Development of a food-grade organogel with high bioaccessibility and loading of curcuminoids. Food chemistry, 131(1), 48-54.
Çirpanli, Y., ünlü, N., Çaliş, S., & Atilla Hincal, A. (2005). Formulation and in-vitro characterization of retinoic acid loaded poly (lactic-co-glycolic acid) microspheres. Journal of microencapsulation, 22(8), 877-889.

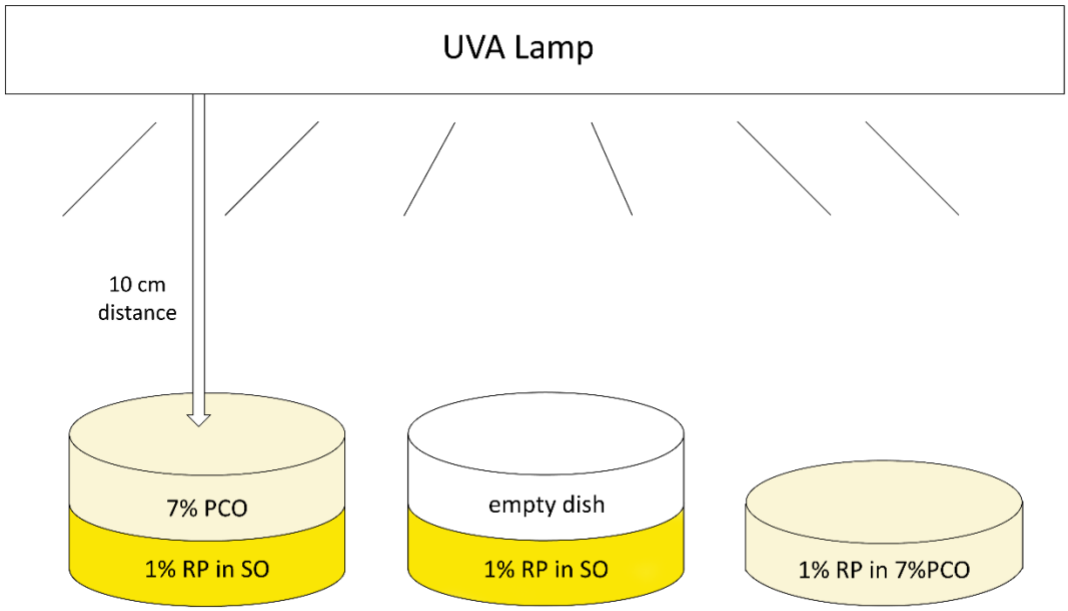

Figure 3.1 Diagram showing experimental setup of the UVA block study

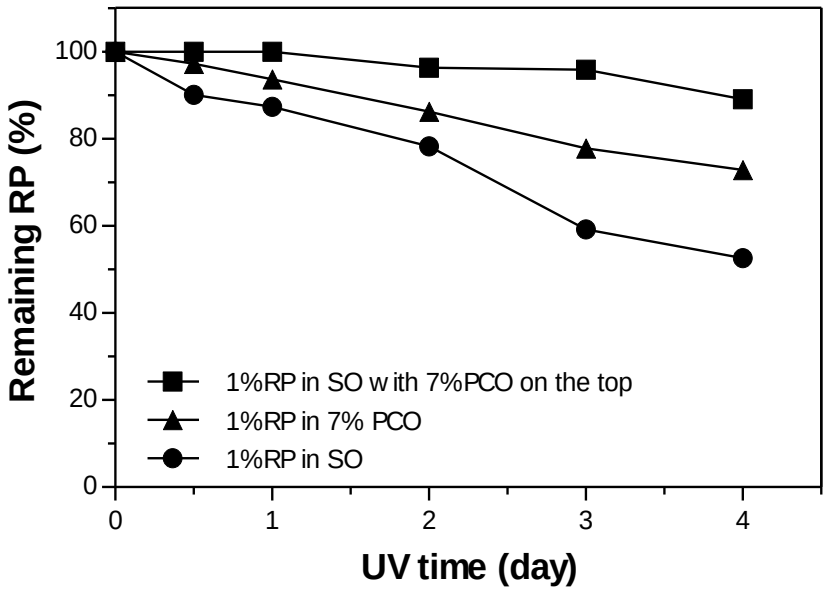

Figure 3.2 Remaining RP (%) values in SO with 7% PCO (w/w) on the top and 1%RP in 7% PCO after different times (0, 0.5, 1, 2, 3, 4 days) of UVA radiation. 1% RP in soybean oil is shown in the figure as control.

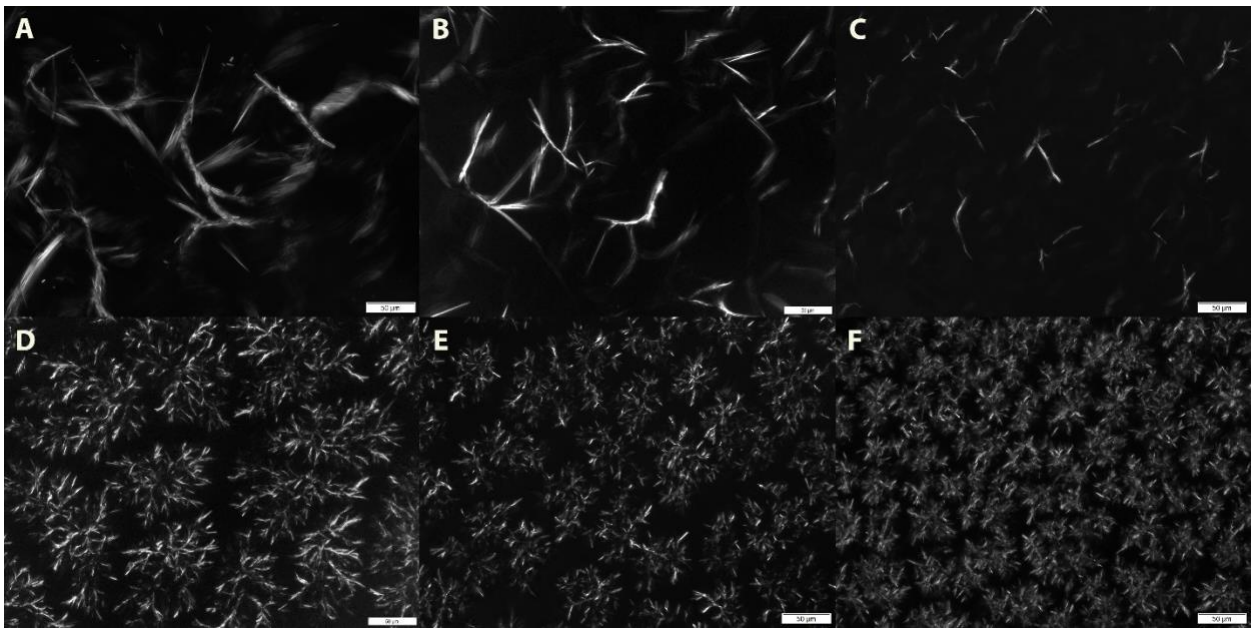

Figure 3.3 Micrographs obtained by DIC microscope of 7% and 12% PCOs (w/w) prepared at different cooling rate: (A) 7% PCO, 2°C/min (B) 7% PCO, 8°C/min (C) 7% PCO, 25°C/min (D) 12% PCO, 8°C/min (E) 12% PCO, 14°C/min (F) 12% PCO, 25°C/min

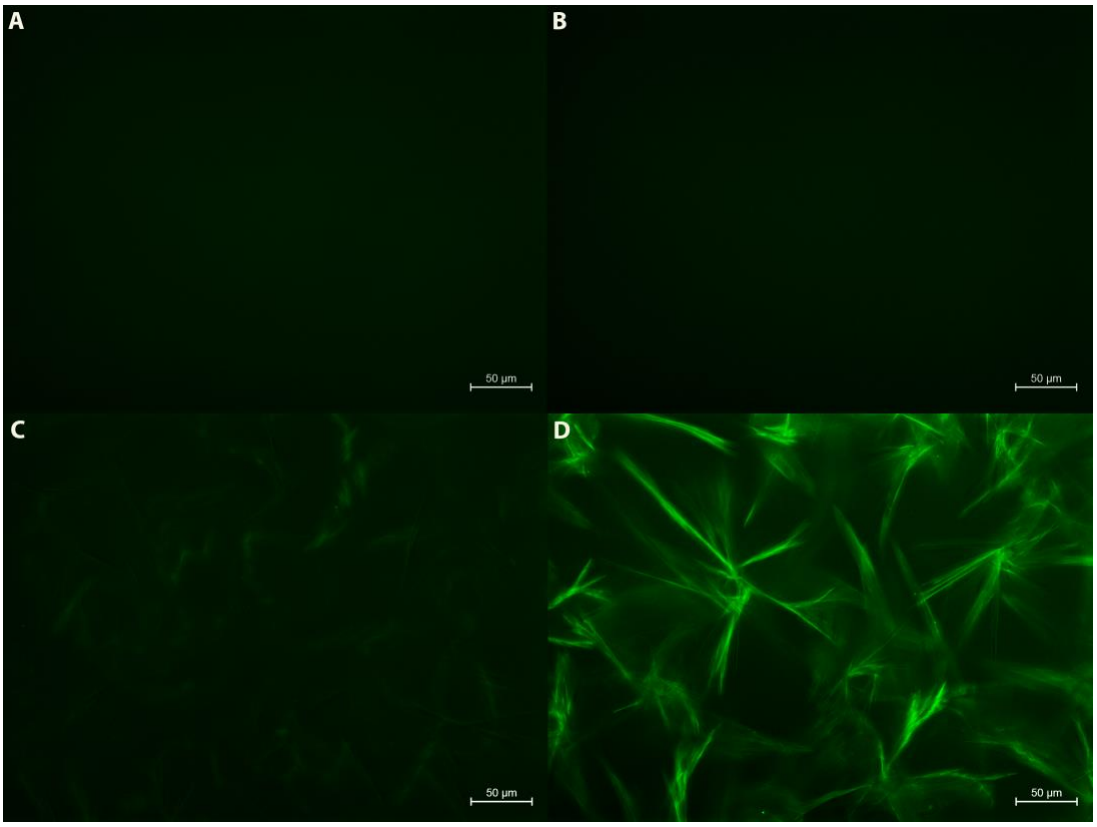

Figure 3.4 Fluorescence micrographs of (A) SO (B) 1% RP in SO (C) 7% PCO (w/w) (D) 7% PCO with 1% RP

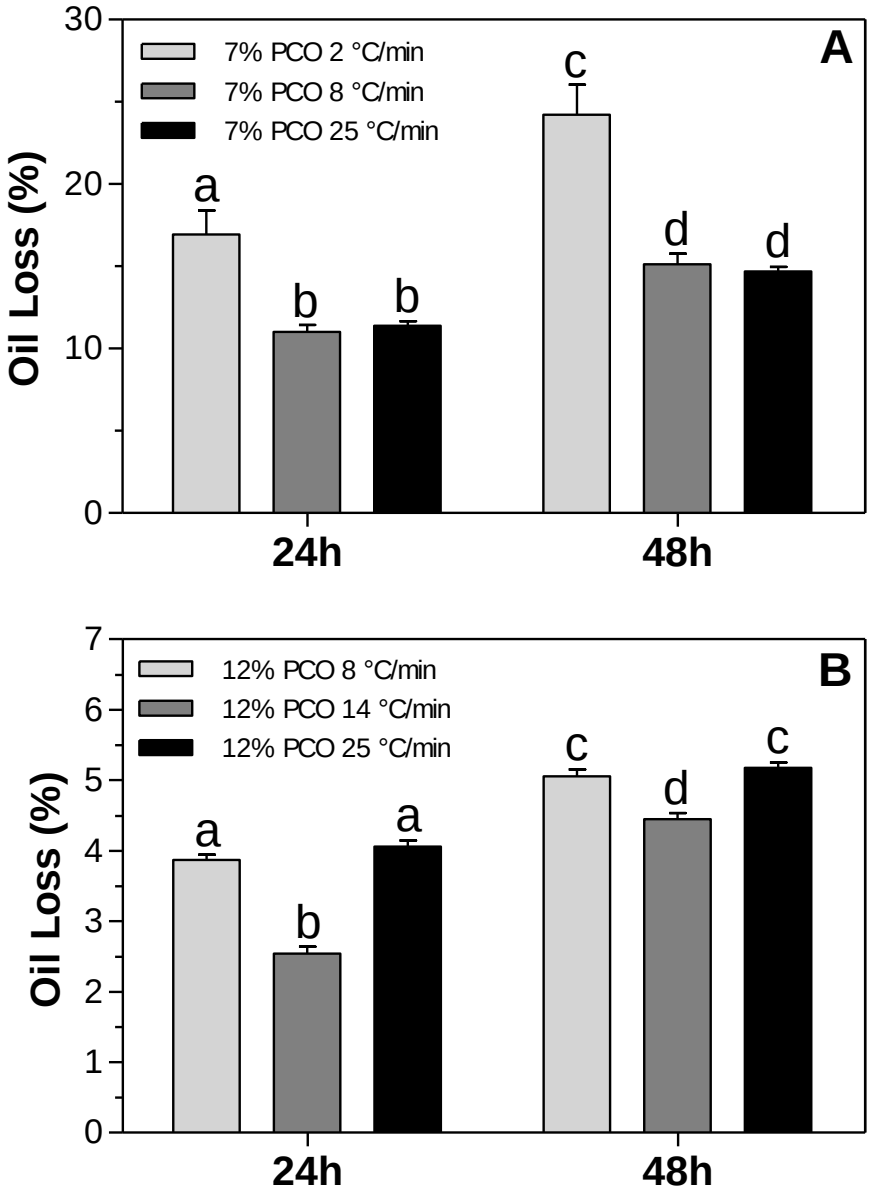

Figure 3.5 Oil loss values (% OL) for (A) 7% and (B) 12% PCOs (w/w) prepared at different cooling rate. Different letters assigned to each bar represent statistically significant differences between the values across all samples ($p < 0.05$).

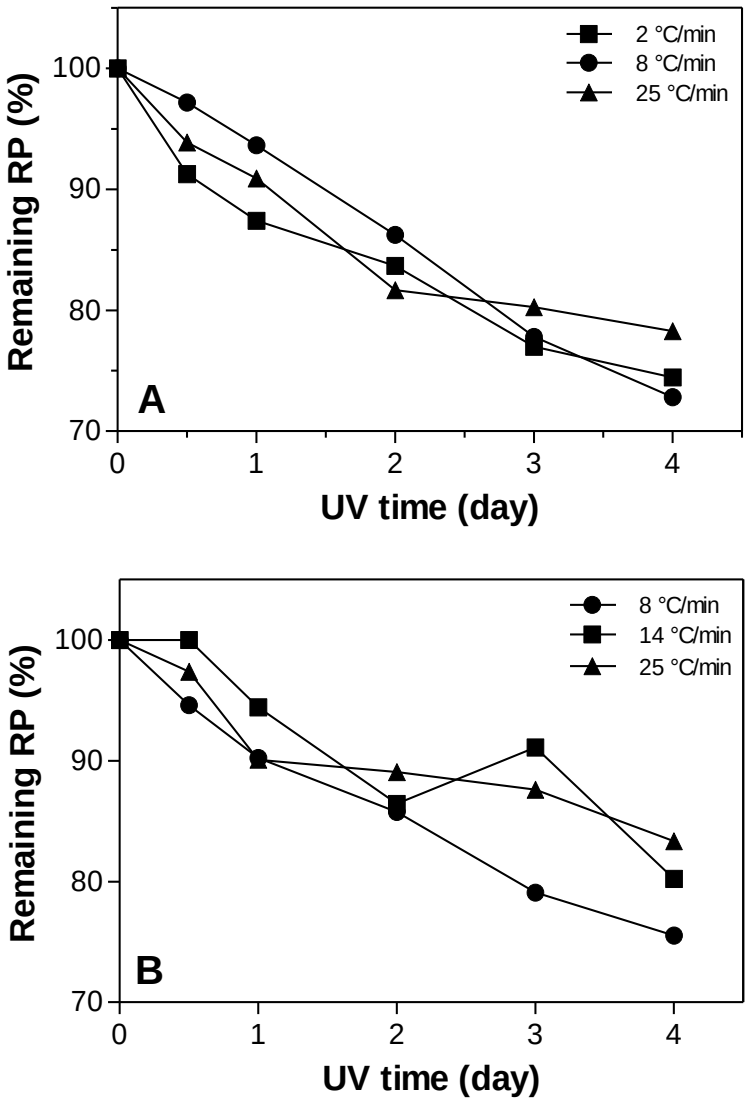

Figure 3.6 Remaining RP (%) values in (A) 7% and (B) 12% PCOs (w/w) prepared at different cooling rate after different times (0, 0.5, 1, 2, 3, 4 days) of UVA radiation.

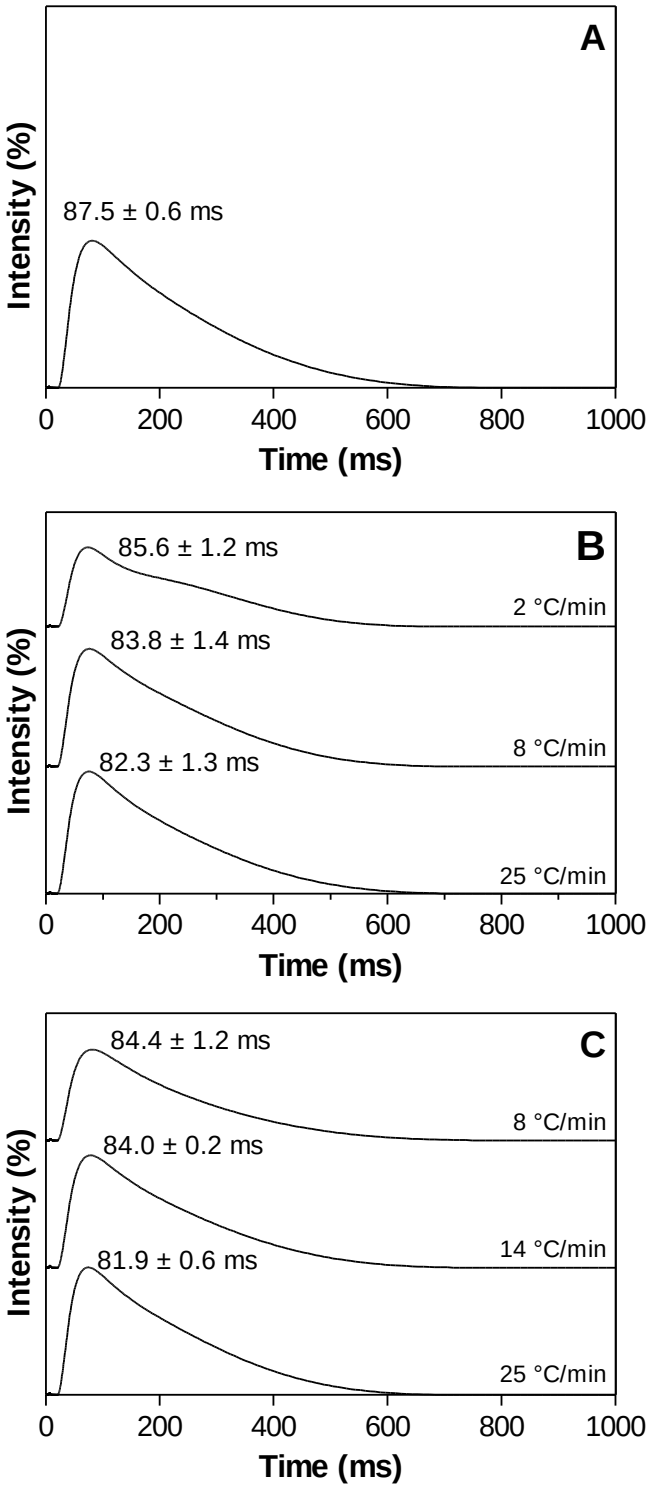

Figure 3.7 NMR T2 relaxation spectra of SO and PCO samples prepared at different cooling rates: (A) SO (B) 7% PCO (C) 12% PCO

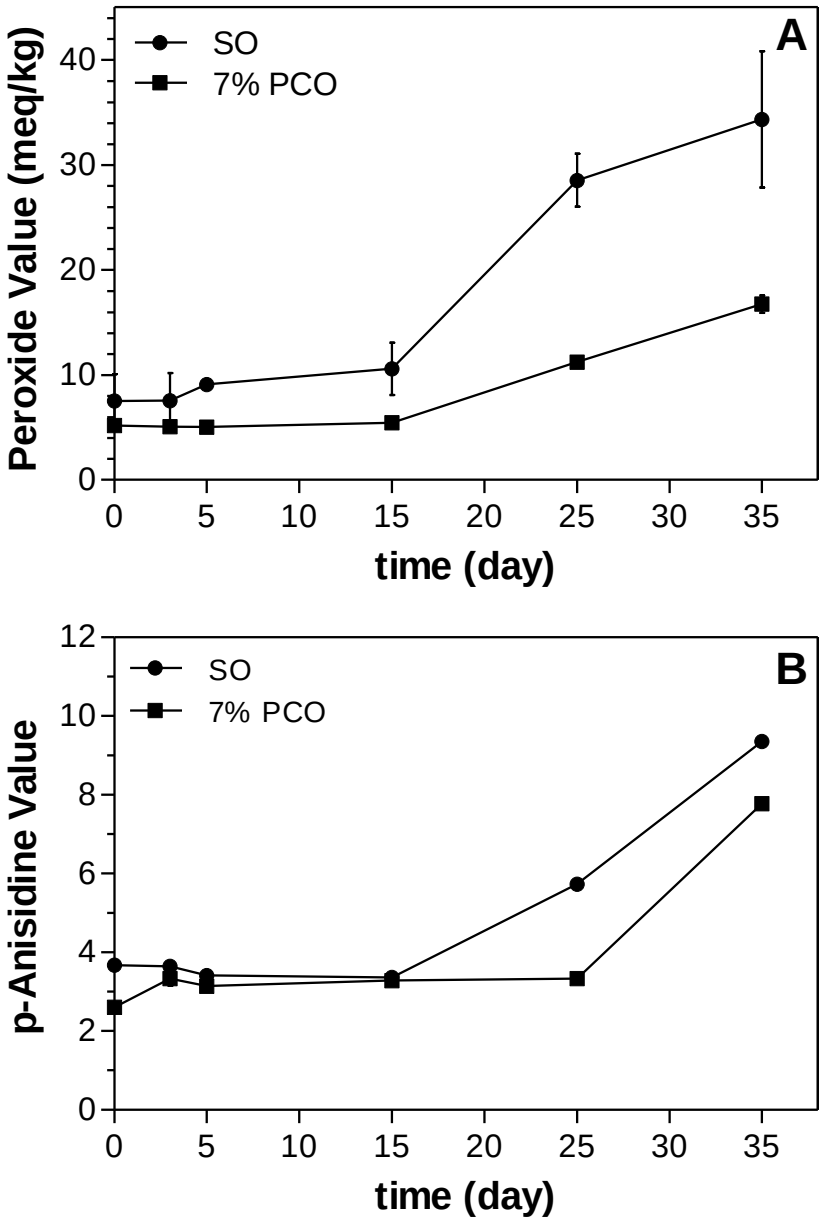

Figure 3.8 PV and p-A.V. of SO and 7%PCO incubated at 40 °C over time

CHAPTER 4. GENERAL CONCLUSIONS

The overall objective of this research was to study the photostability of retinyl palmitate (RP) entrapped in policosanol oleogesls (PCO) and its photoprotective mechanism. The first study (Chapter 2) focused on the characterization of semi-solid PCOs and PCOs as matrix to protect RP from UVA mediated photodegradation. It was found that with the increase of PC concentration, the gelation temperature and gel strength increased, where matrix mobility decreased. The HPLC results showed that PCOs efficiently protected RP from UVA-mediated degradation, where over 75% of RP activity remained after 4 days of UVA irradiation in PCOs. *cis*-RP isomer, with less than 75% all *trans*-RP activity, was found in liquid soybean oil. PCOs protected RP from isomerization that *cis*-RP was not formed in PCOs. Regardless of RP and policosanol concentration, RP photodegradation followed a 2nd order reaction in PCOs. From the reaction kinetics, it would be possible to predict the RP photodegradtion rate in PCO matrices and engineer PCOs to reach desirable RP protection. The larger the amount of RP added into PCO matrices the more effective the photoprotection exerted by PCOs.

The second study (Chapter 3) investigated the photoprotective mechanism of PCOs on RP. From the UVA block study, it was found that PCOs can efficiently protect RP from UVA mediated photodegradation through physical UV-blocking action. Cooling rate processing played a significant role in the formation of PCOs structure. At higher cooling rate, smaller crystal particles were formed in 7% and 12% PCOs prepared, which provided better RP protection. Florescence microscopy showed that RP was located in the boundaries of the crystalline network, which suggested that the crystalline network structure immobilized RP in PCO matrix. The low resolution NMR results supported this result; PCOs

immobilized RP in the network and reduced molecular collision. From the oxidative stability study, it was found that PCOs effectively hinder the progress of radical-mediated oxidative reactions which further contributed to the stability of RP in PCOs.

Overall, we demonstrated that PCO is an efficient oil-structuring strategy to improve RP-photostability with the advantages of low cost, high protection efficiency, long-term system stability and simple preparation. It protects RP from photodegradation through a combined effect of physical UV-barrier action, molecular immobilization and inhibition of the free radical-mediated reaction. PCOs enriched in RP have shown functional properties, which are desirable for food and cosmetic applications.

Future work

Future research can focus on exploring the release properties of PCOs as oral delivery system of lipophilic agents, such as RP. It would be beneficial to investigate *in vitro* bioaccessibility of RP in PCOs by conducting simulated gastric and intestinal digestion study. Diffusion coefficient should be measured by using NMR to better investigate the molecular immobilization in PCO matrices. Thermal and chemical stability of RP in PCO should be measured to better explore potential applications of RP-PCO in food products, medical treatment and cosmetics products. Electron spin resonance (ESR) spectroscopy can be used to directly measure free radical species involved photodegradation of RP in PCO. LCMS can be used to identify the photoreaction products of RP in PCOs.

Different formulas of oleogel gelator can be studied to reach desirable properties, such as using fatty acid and policosanol mixture to lower total gelator concentration in oleogel. On the other hand, self-assembled oleogles, such as beta-sitosterol and gamma-oryzanol oleogel, can be developed to protect RP from photodegradation.